An Overview of Plasmasphere Dynamics II:

Plasmasphere/Ionosphere Coupling

Jonathan Krall

Retired (formerly of Naval Research Laboratory, Plasma Physics Division)

International School of Space Science

September 26, 2022

Some Credits

NRL Plasma Physics Division	Joseph Huba (now at Syntek)
NRL Space Science Division	John Emmert Doug Drob
Also	Richard Denton (Dartmouth U.) Mei-Ching Fok (NASA/GSFC) Geoff Crowley (ASTRA) Mark Moldwin (U. Michigan) Daniel Weimer (VA Tech)

Outline

I. 'Cold' and 'energetic' plasma

II. Thermosphere winds shape the plasmasphere

III. Thermosphere densities affect H^+ outflow

IV. Ring current heating and the O^+ torus

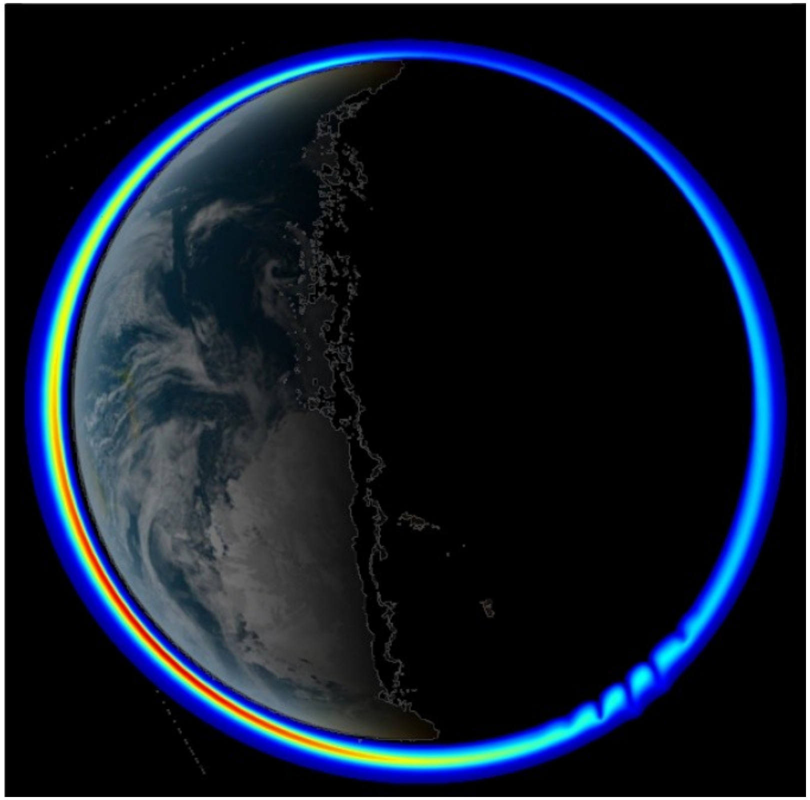

Huba and Joyce, GRL, 2010

Throughout, we will look for interesting unsolved problems

I. ‘Cold’ and ‘energetic’ plasma

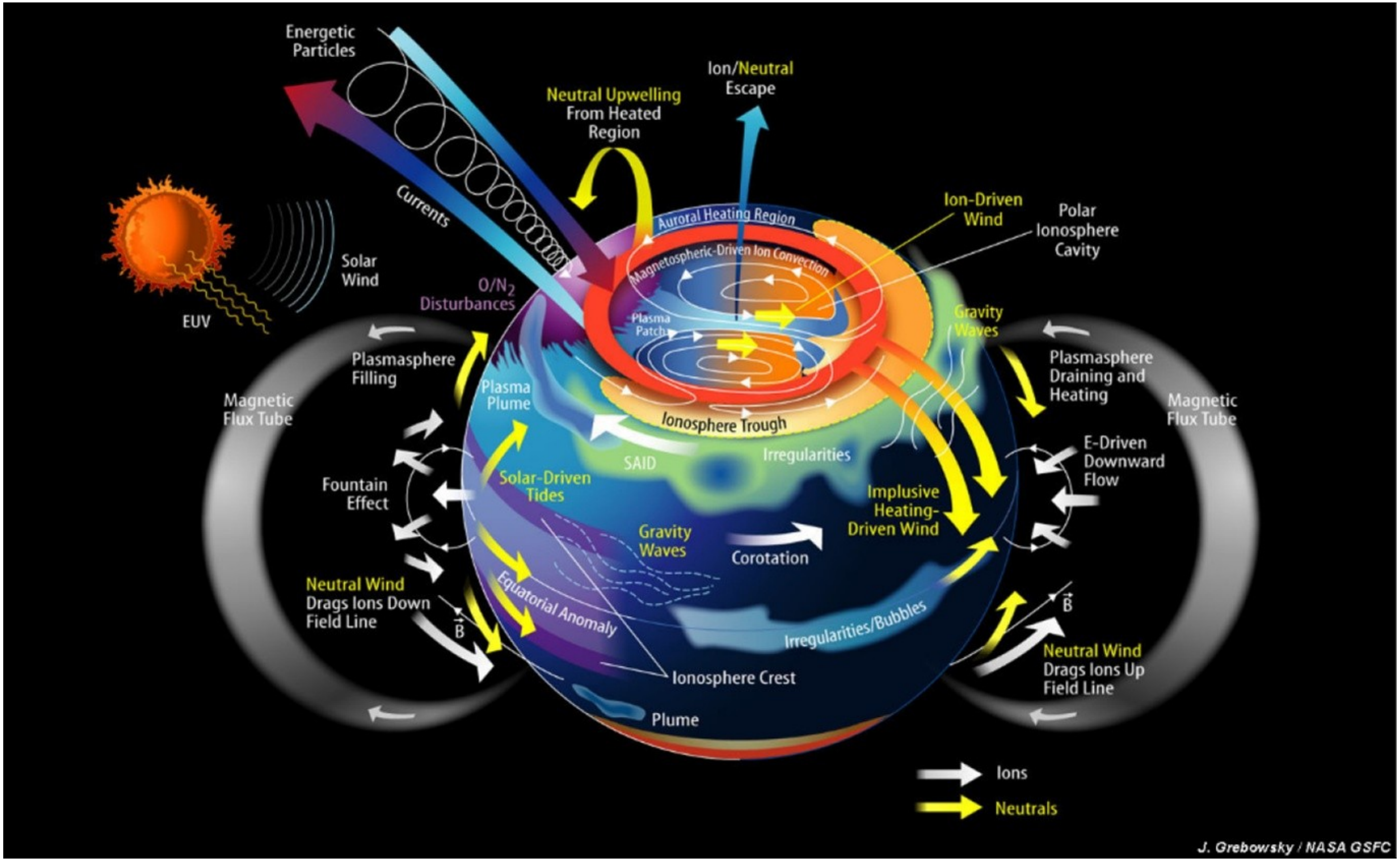

‘Cold’ plasma is too cold to be detected by a mass spectrometer on a spacecraft without spacecraft charging control. Cold ≈ 1eV ≈ 10^4K

‘Cold’ plasma outflows

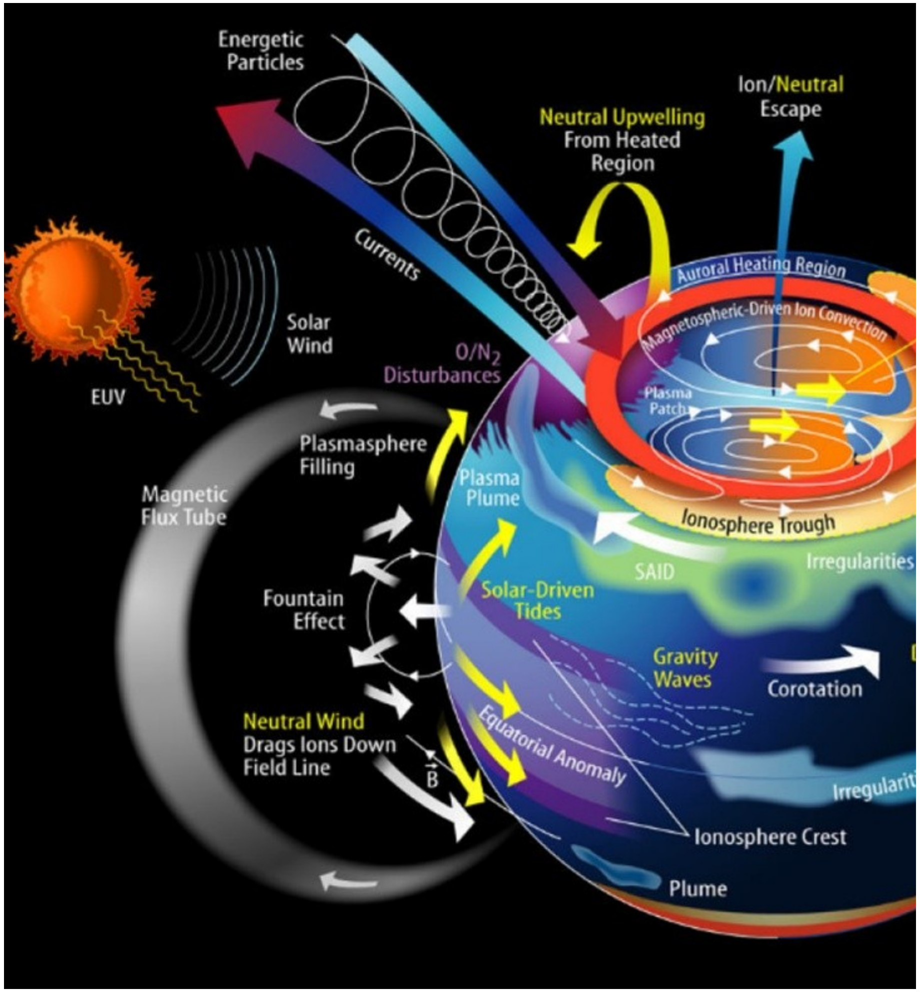

The classical polar wind is an H^+ and He^+ thermal outflow into ‘open’ flux tubes.

H^+/He^+ thermal outflows into closed, co-rotating flux tubes is called refilling.

Recent work suggests that thermal O^+/N^+ outflows are caused by the heating of the plasmasphere by the ring current.

A ‘cold’ (thermal) plasma typically has a Maxwellian temperature

Cold plasma: DE Retarding Ion Mass Spectrometer

DE:RIMS [Horwitz et al., JGR, 1986]

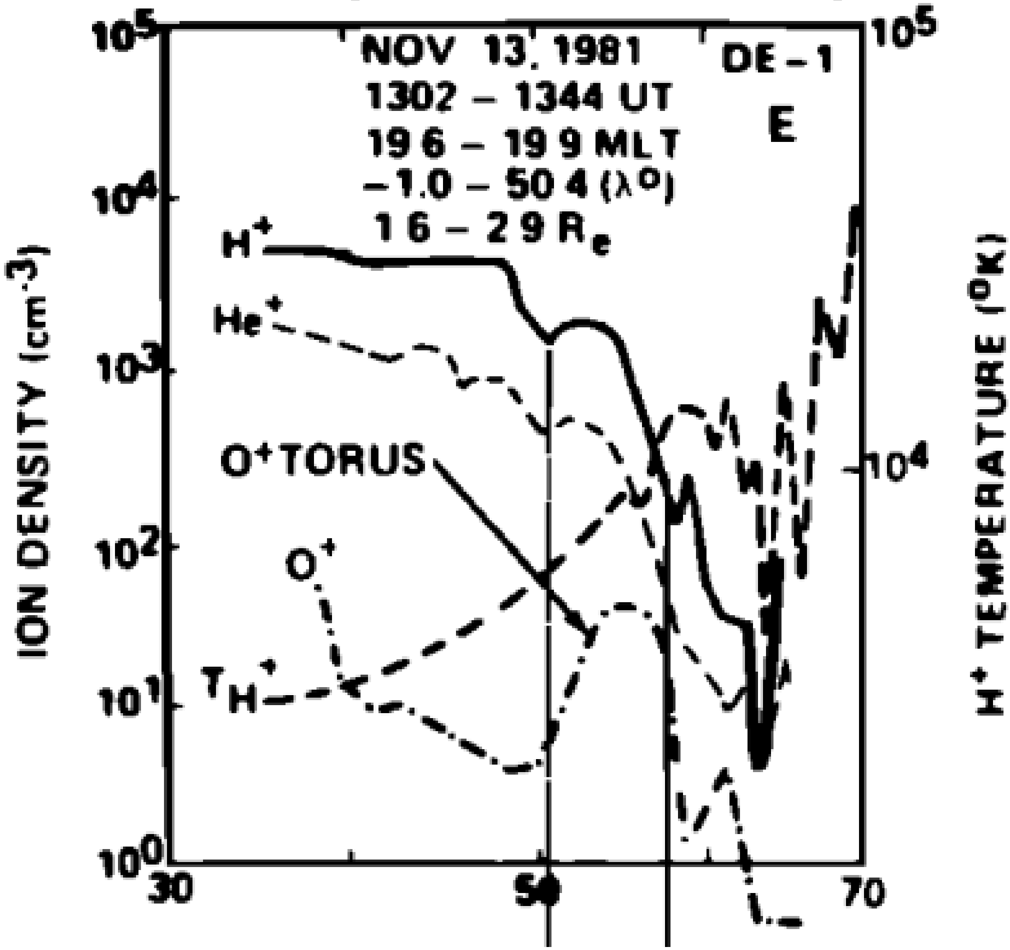

A mass spectrometer with spacecraft charging control last flew in the 1980s, the Dynamics Explorer missions

R. Denton (Dartmouth U.) suggested that these profiles do not capture the full density

Cold plasma: number and mass density measurements

VAP [Nosé et al., JGR, 2015]

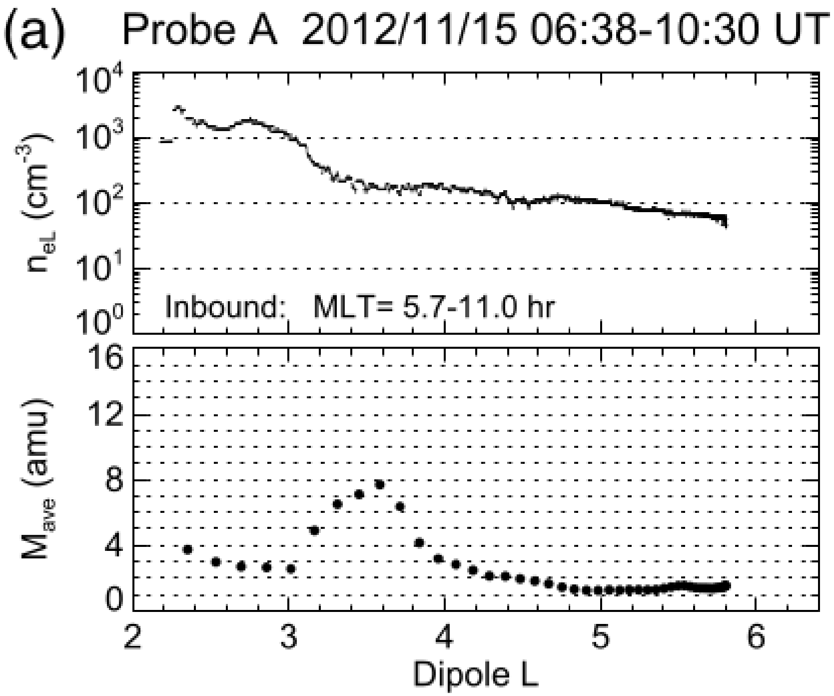

CRRES [Takahashi et al., JGR, 2008]

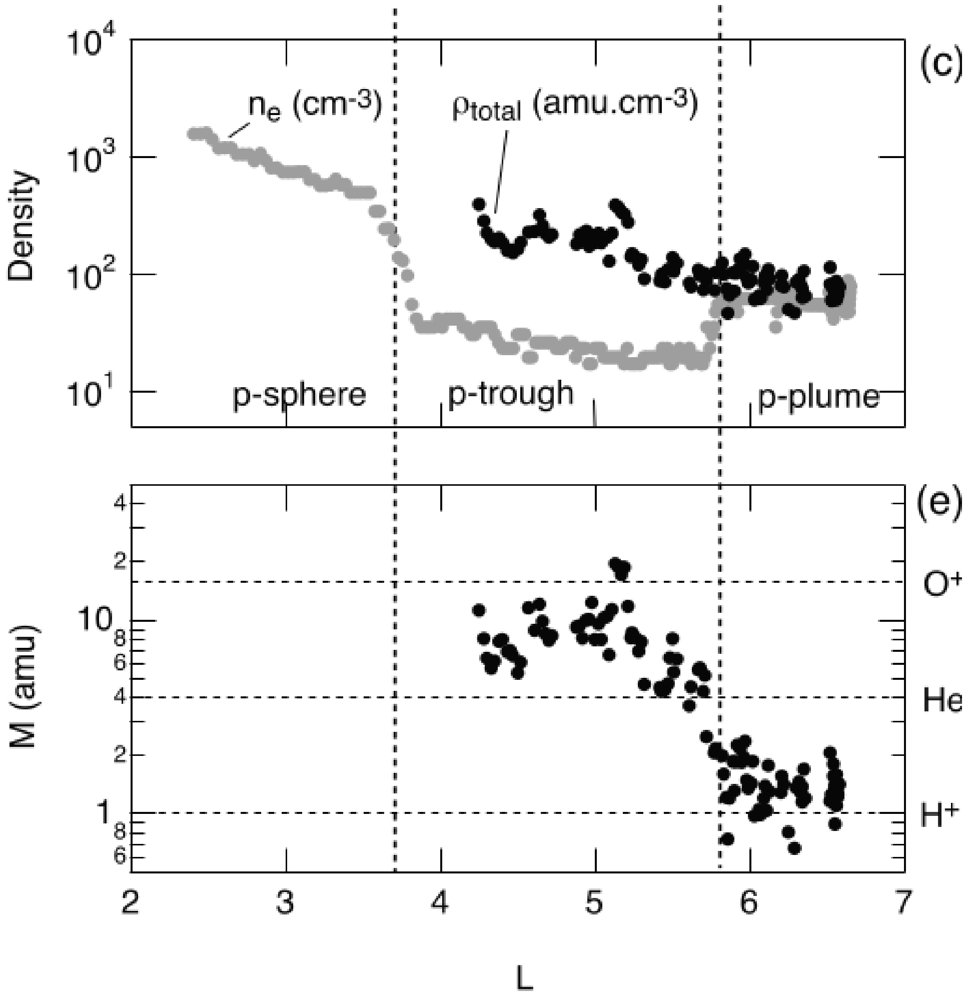

Cold plasma: DE Retarding Ion Mass Spectrometer

[Horwitz et al. JGR, 1986]

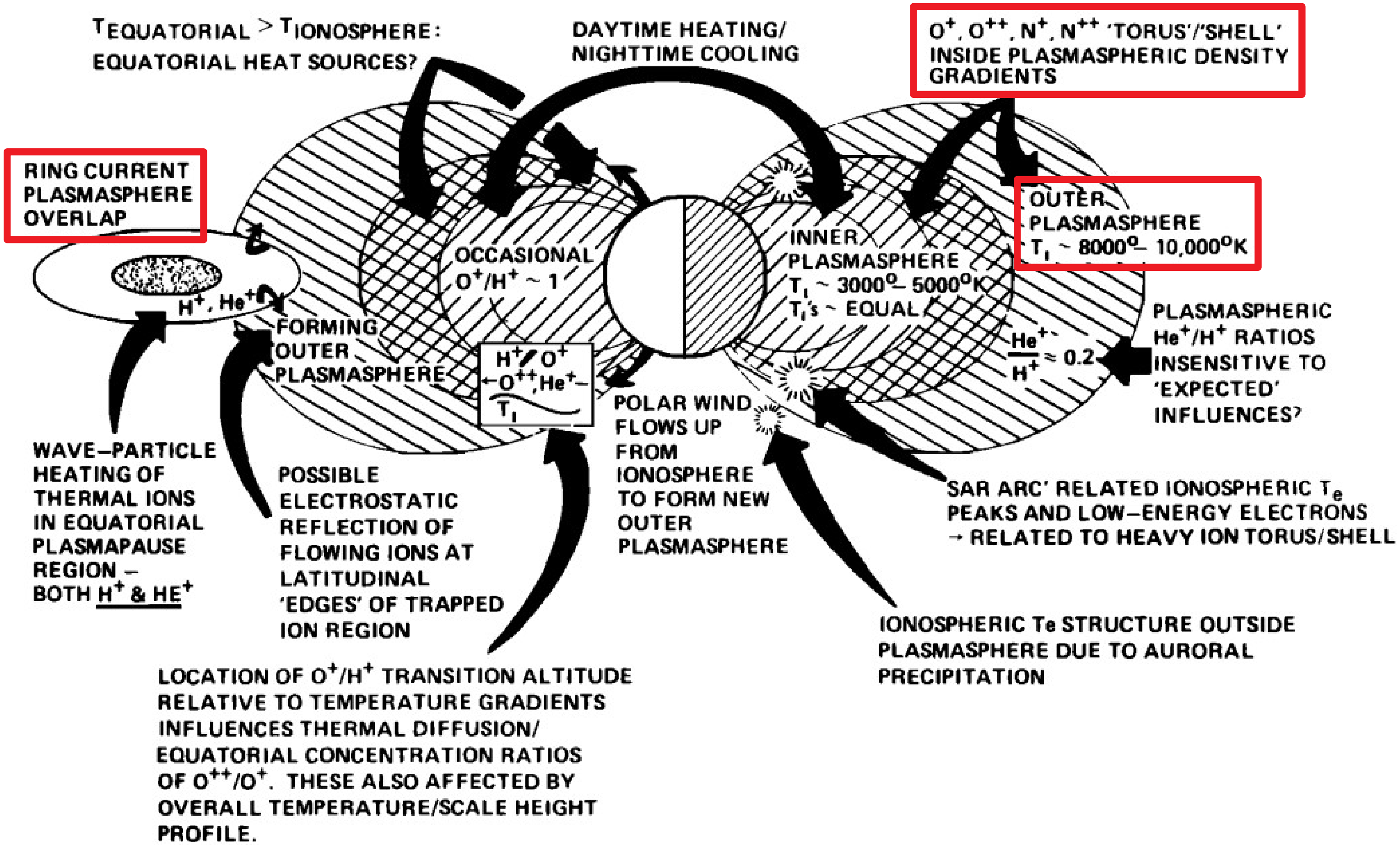

A 'cold' (thermal) plasma typically has a Maxwellian temperature.

The plasmasphere temperature structure is not yet fully explained.

‘Cold’ and ‘energetic’ plasma sources

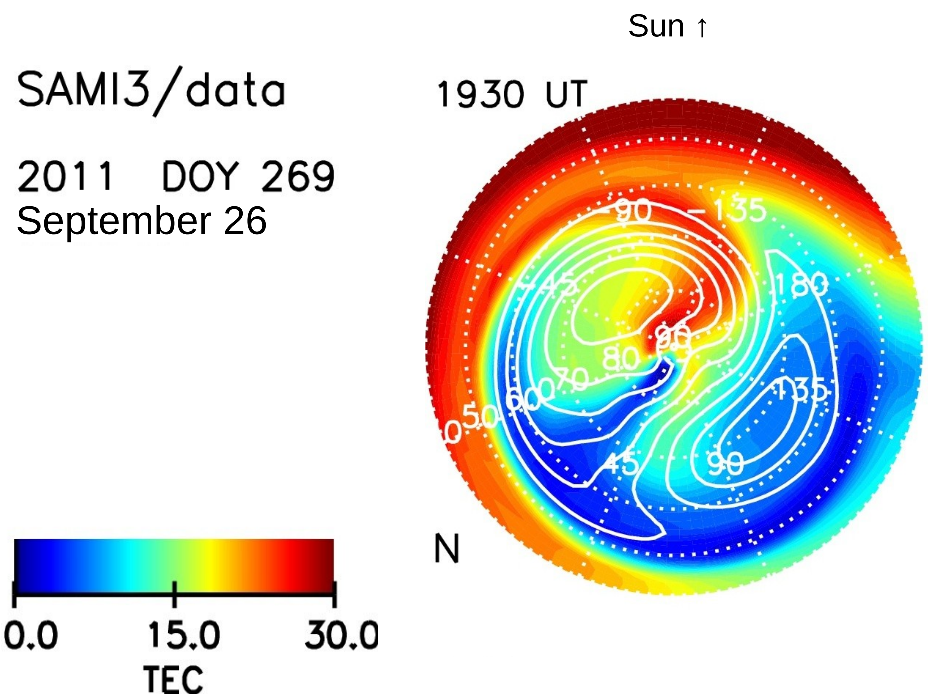

GPS/SuperDARN [Thomas et al., JGR, 2013]

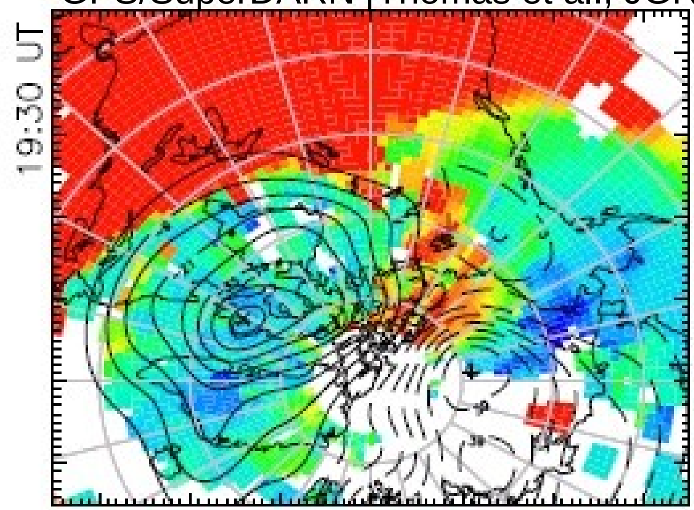

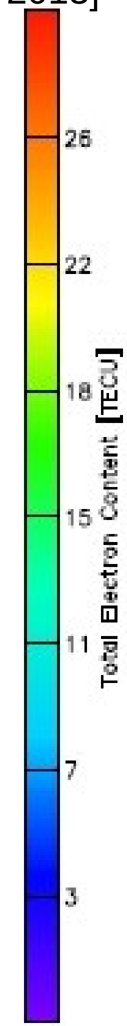

We find evidence that ‘cold’ outflows are associated with ionosphere features, such as the tongue of ionization.

Are ionosphere features associated with the ‘energetic’ ions?

Are energetic ions driven primarily by the magnetosphere?

II. Thermosphere winds shape the plasmasphere

Direct force of winds on the ionosphere:

$$\frac{\partial \mathbf{V}_i}{\partial t} + \mathbf{V}_i \cdot \nabla \mathbf{V}_i = -\frac{1}{\rho_i}\nabla \mathbf{P}_i + \frac{e}{m_i}\mathbf{E} + \frac{e}{m_i c}\mathbf{V}_i \times \mathbf{B} + \mathbf{g}$$

$$-\nu_{in}(\mathbf{V}_i - \underline{\mathbf{V}_{\mathbf{n}}}) - \sum_j \nu_{ij}\left(\mathbf{V}_i - \mathbf{V}_j\right)$$

Wind-driven dynamo:

$$\nabla \cdot \Sigma \nabla \Phi = S(g, \underline{V_n}, J_{||})$$

$$\mathbf{E} = -\nabla \Phi$$

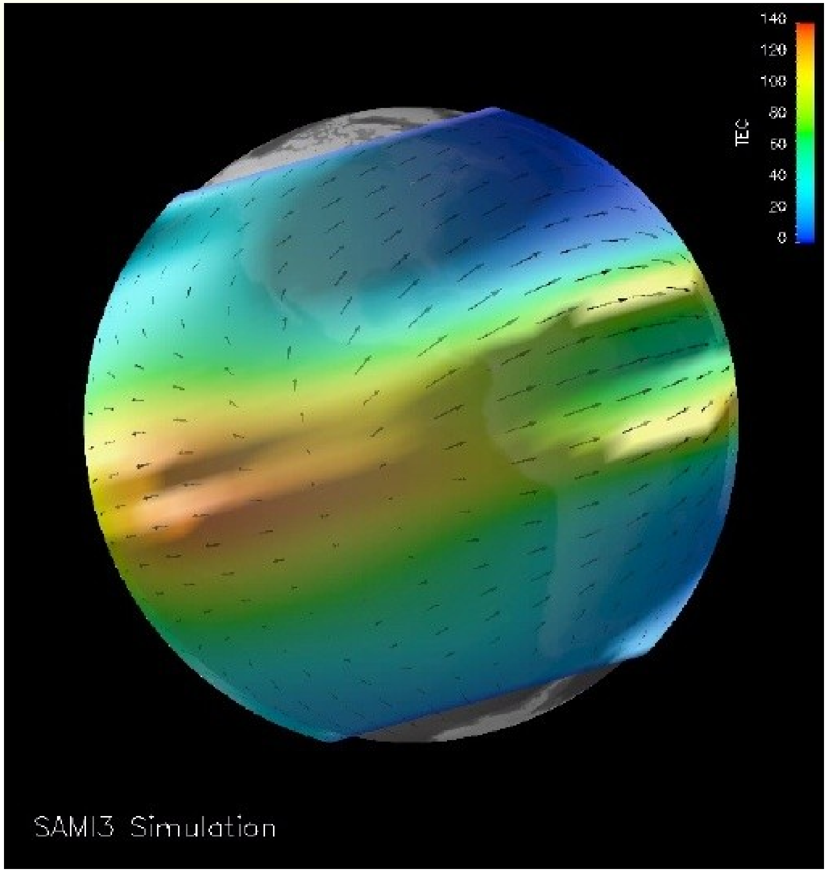

SAMI3: 2001 Day 32-36, quiet post-storm refilling

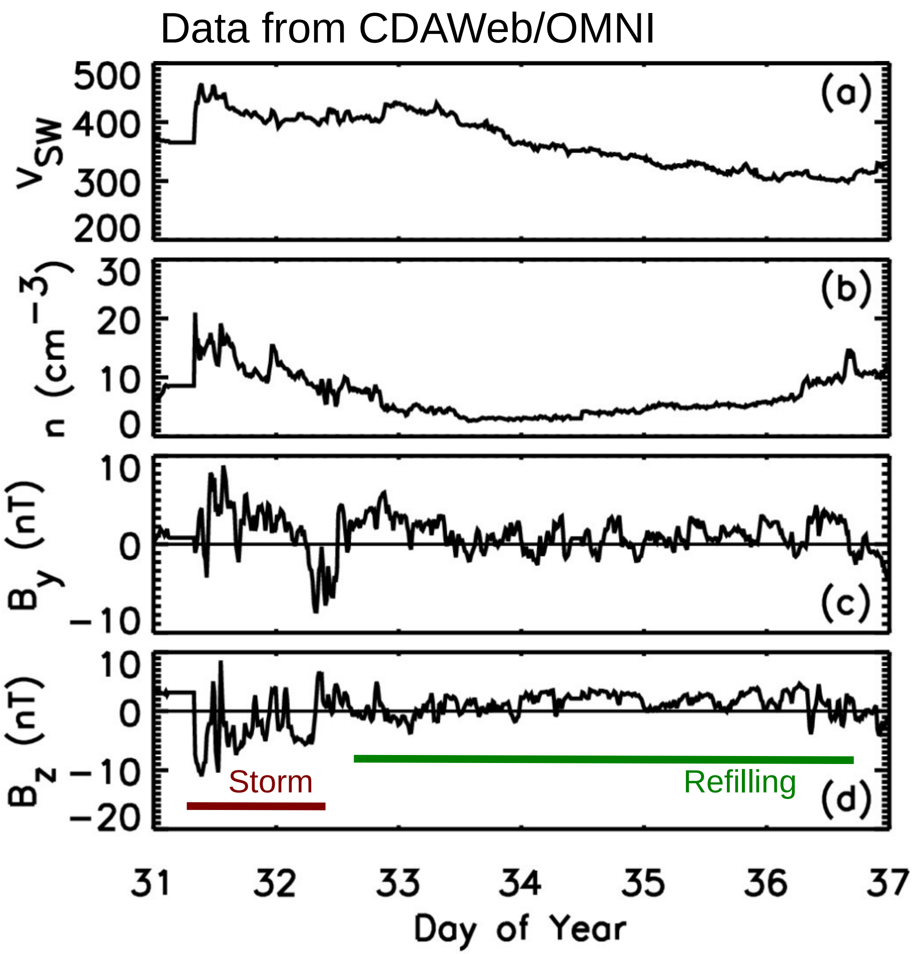

SAMI3/Weimer 7-day run:

- 1 quiet day (day 30)
- 2 storm days
- 4 refilling days (day 33-36)

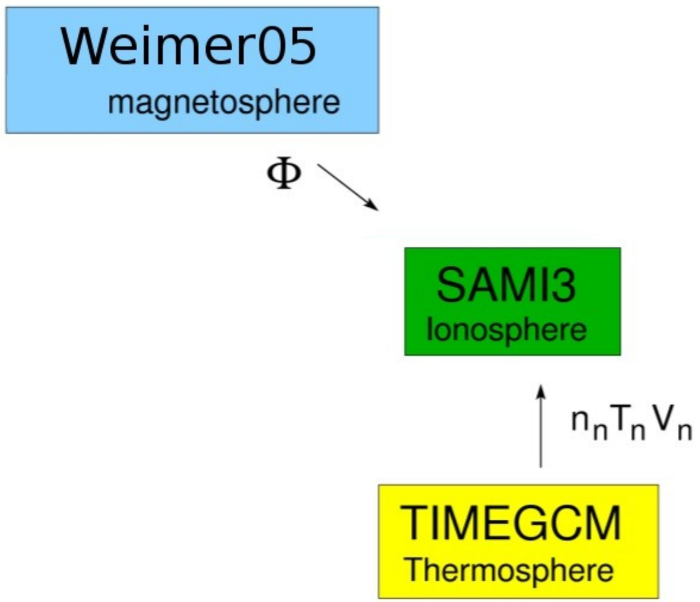

[Krall et al., JGR, 2014]

2001 Day 32-36: three different wind models

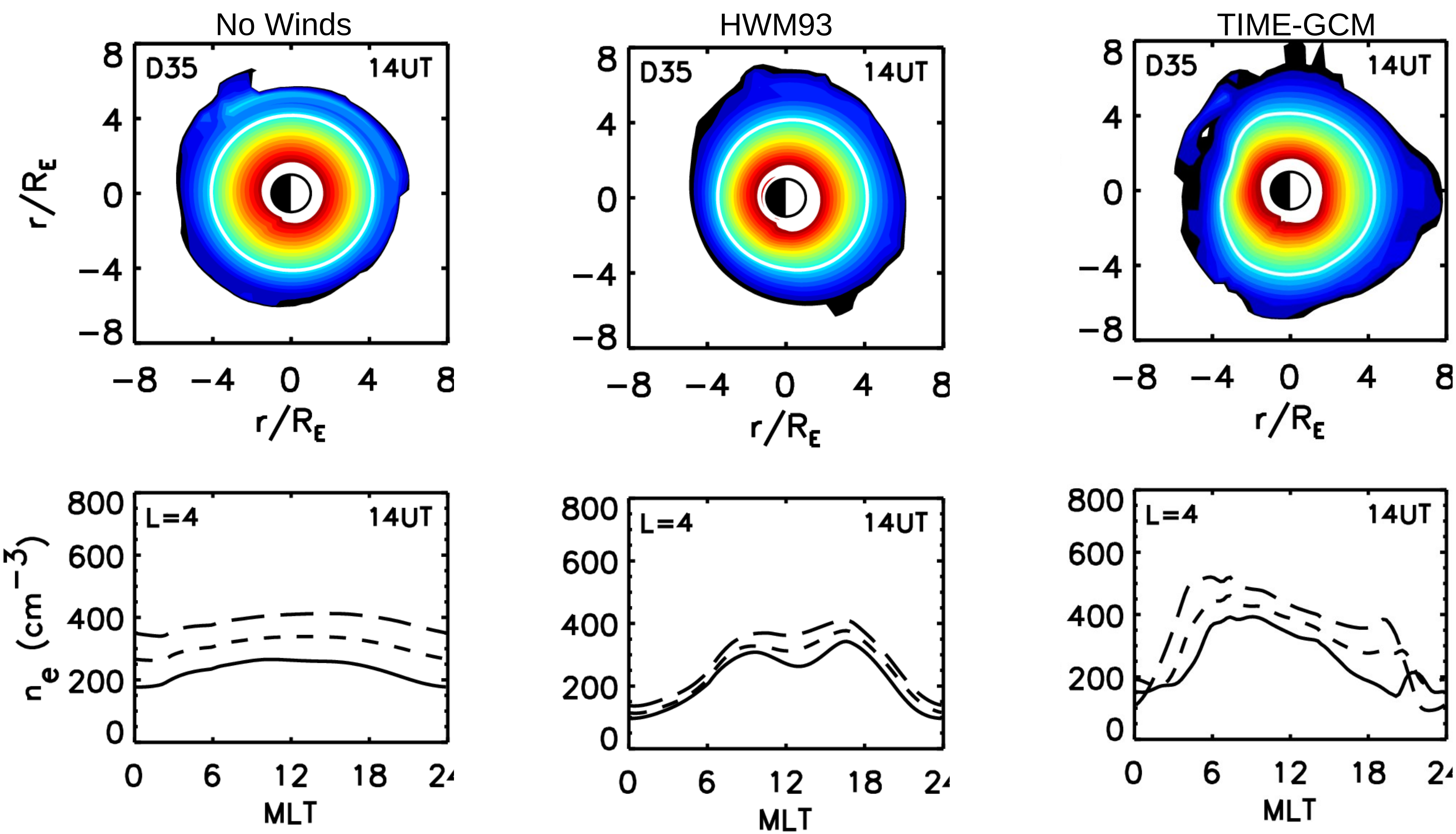

The plasmasphere shape is affected by winds in the thermosphere.

2001 Day 32-36: SAMI3 with HWM93

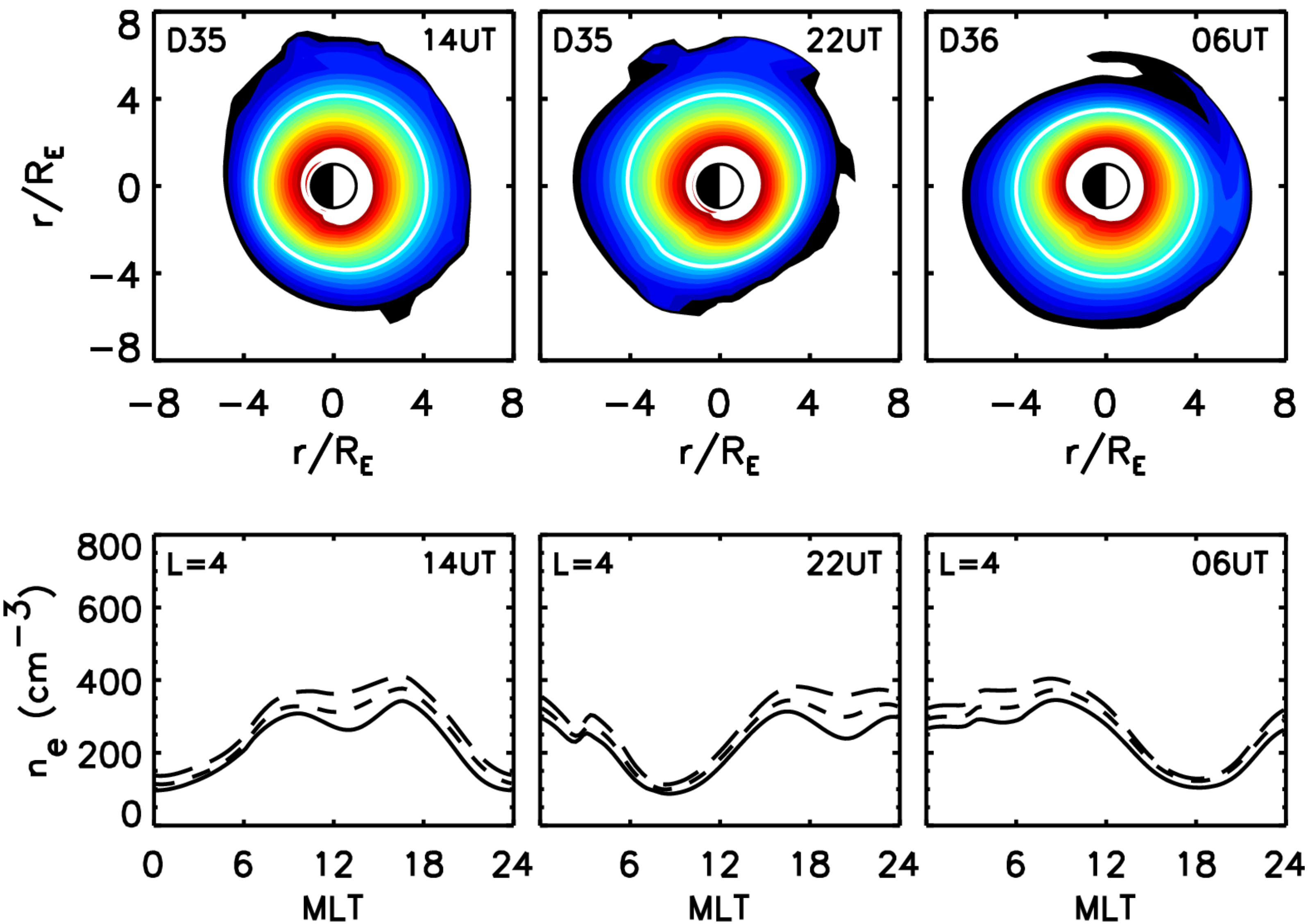

Spatial extent of the wind effect

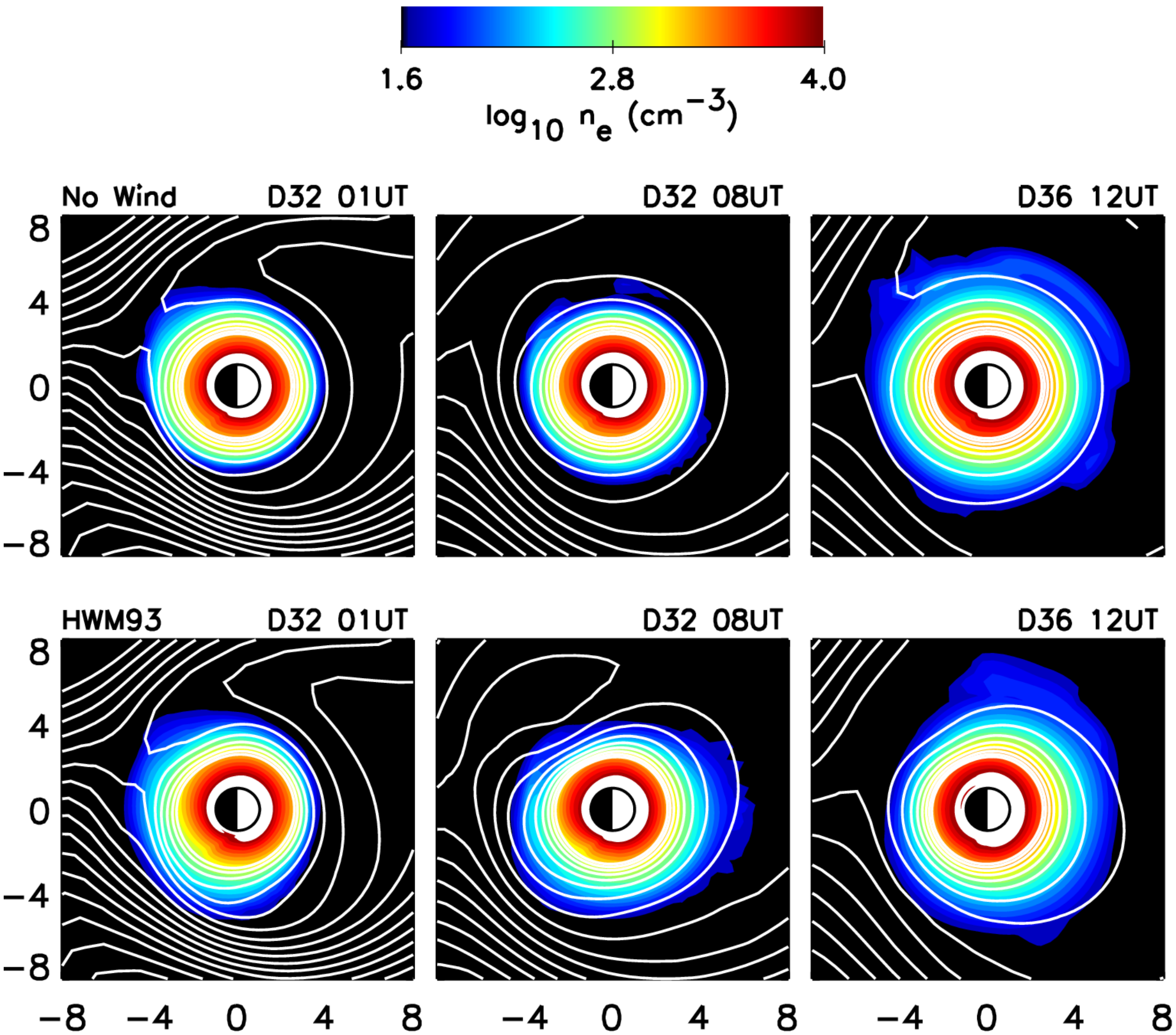

Winds affect the potential out to L=4 during a storm and out to L=6 during quiet times.

2001 Day 32-36: IMAGE/RPI electron density

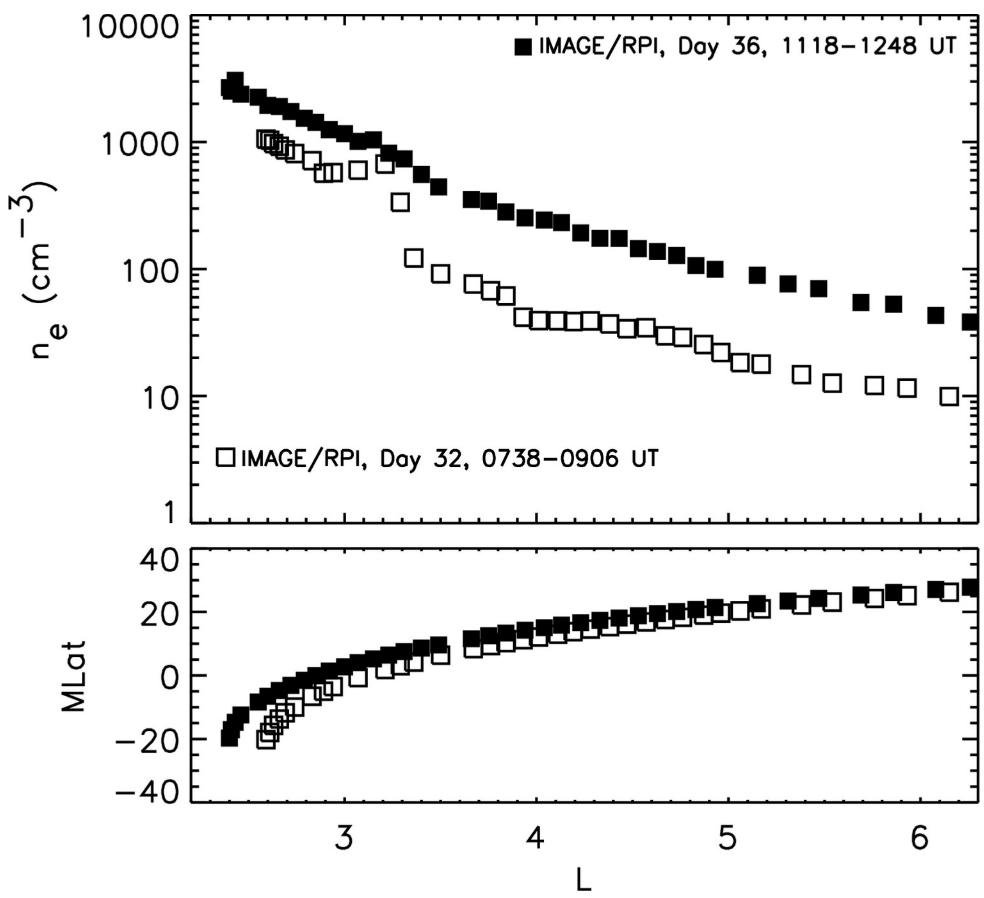

RPI on the IMAGE satellite measured electron density on each pass through the plasmasphere.

Shown are two passes. Day 32 (eroded) and day 36 (refilled).

Data/analysis: Richard Denton

SAMI3 test of two wind effects

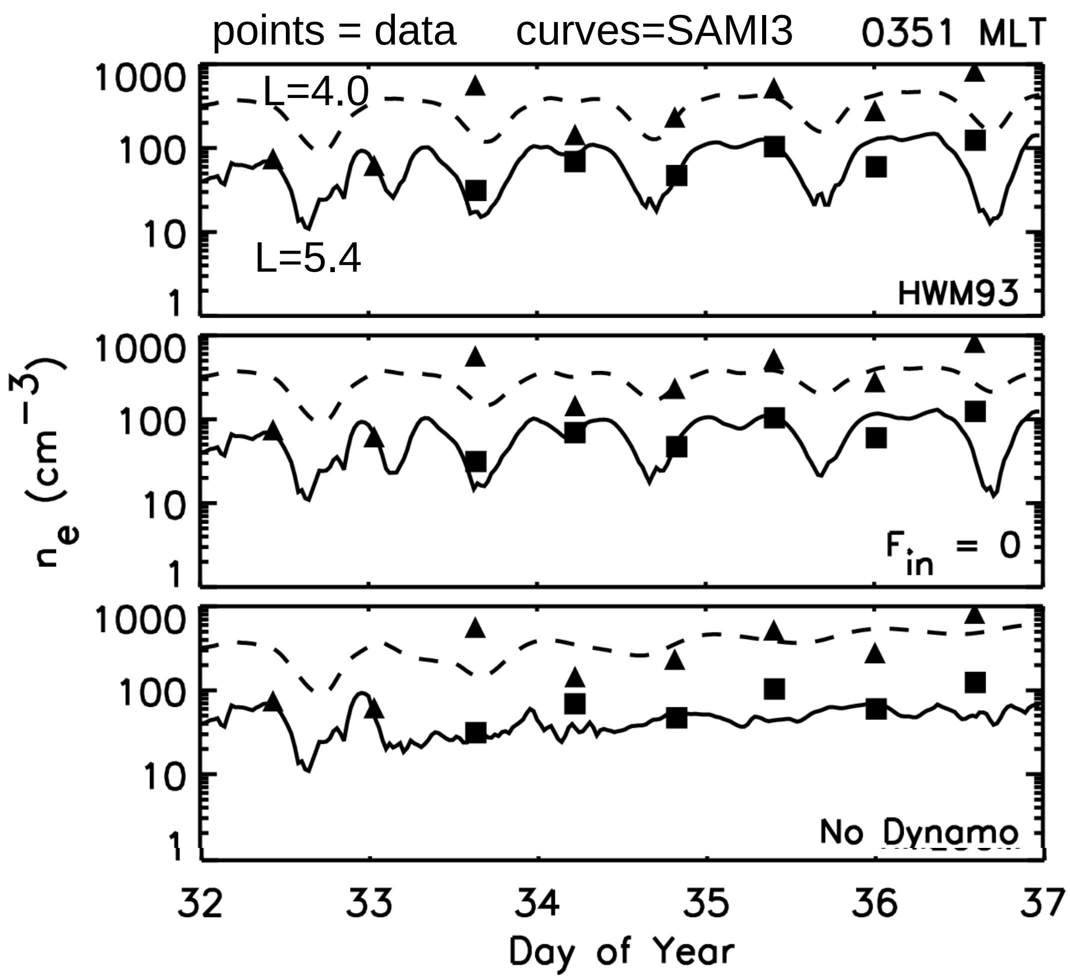

IMAGE/RPI densities are at MLT 03:50.

1. SAMI3 with HWM93

2. Without the ion-neutral force, the oscillations persist.

3. Oscillations are gone in the “No Dynamo” case.

The oscillations have not been confirmed using data.

Winds affect the refilling rate

IMAGE/RPI data and analysis

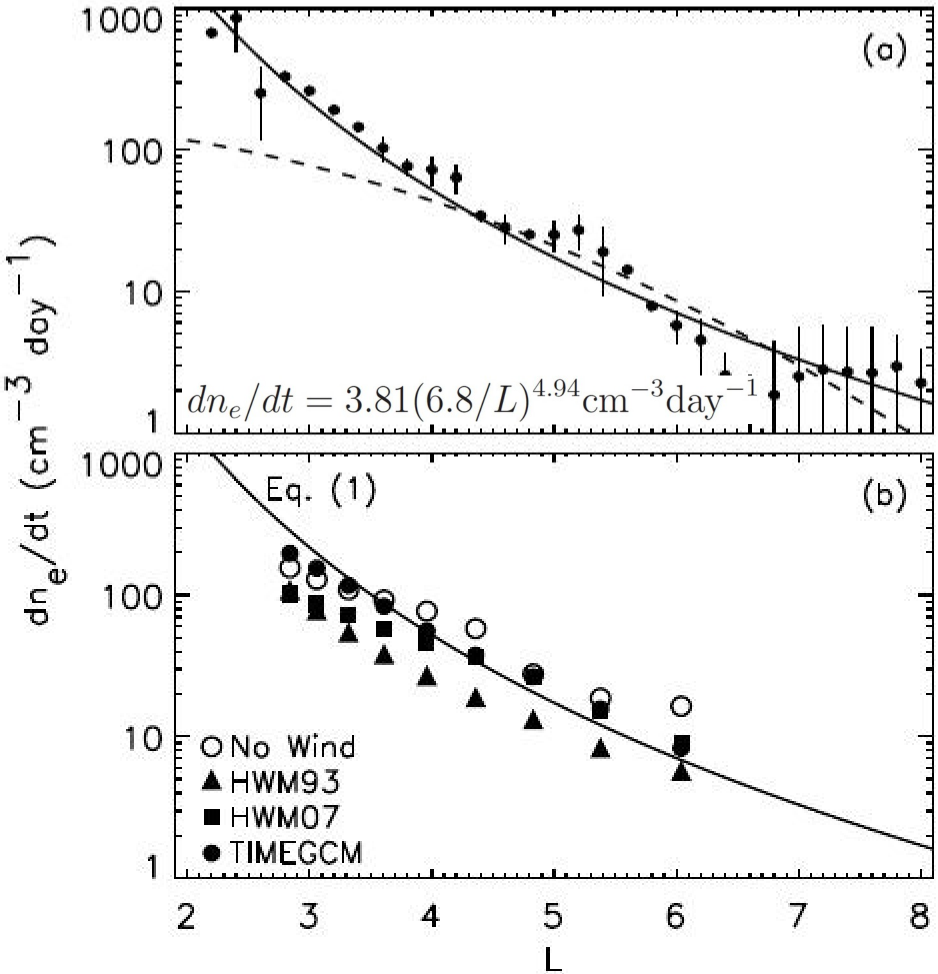

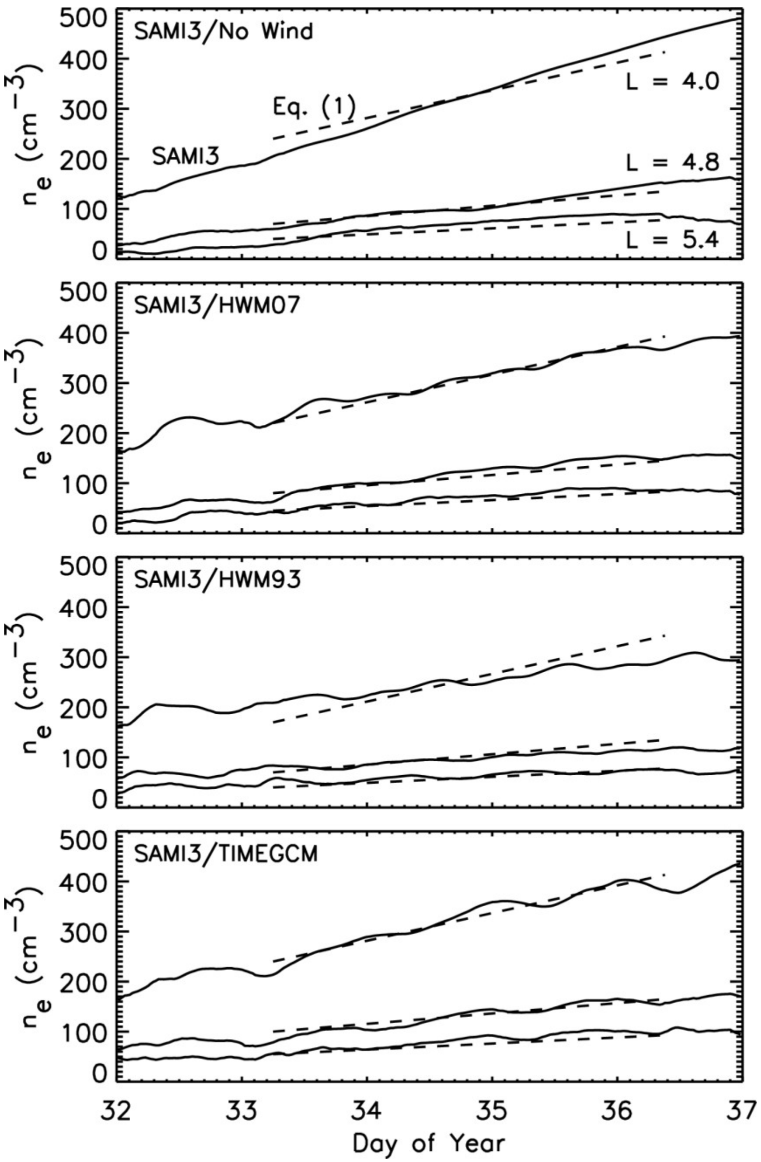

[Krall et al., JGR, 2014]

2001 Day 32-36: TEC

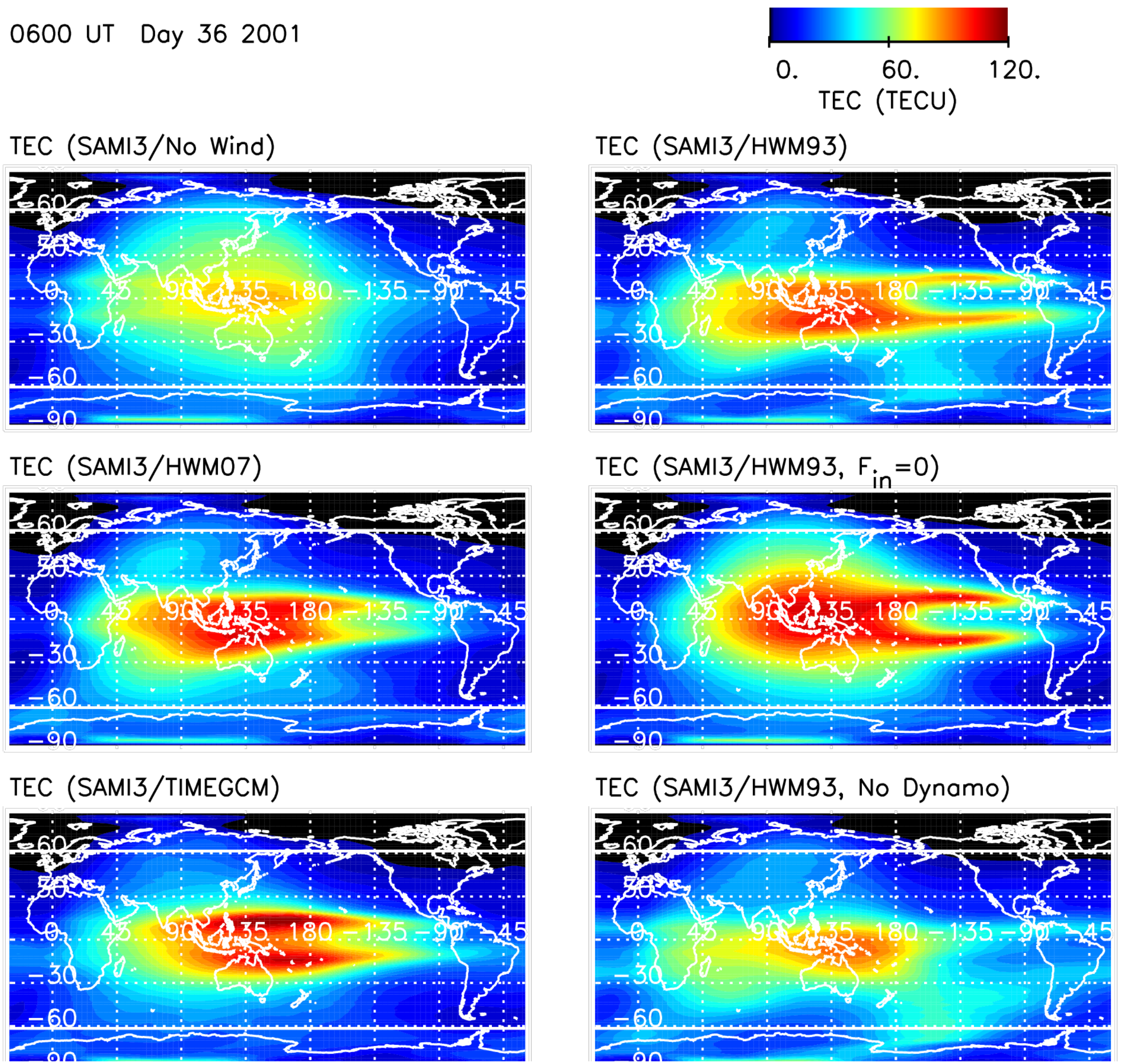

At this time, TEC and the ion fluxes at L=4.8 are larger with no winds or no dynamo.

Ionosphere dynamics continually change the strength of the refilling source.

III. Thermosphere densities affect H^+ outflow

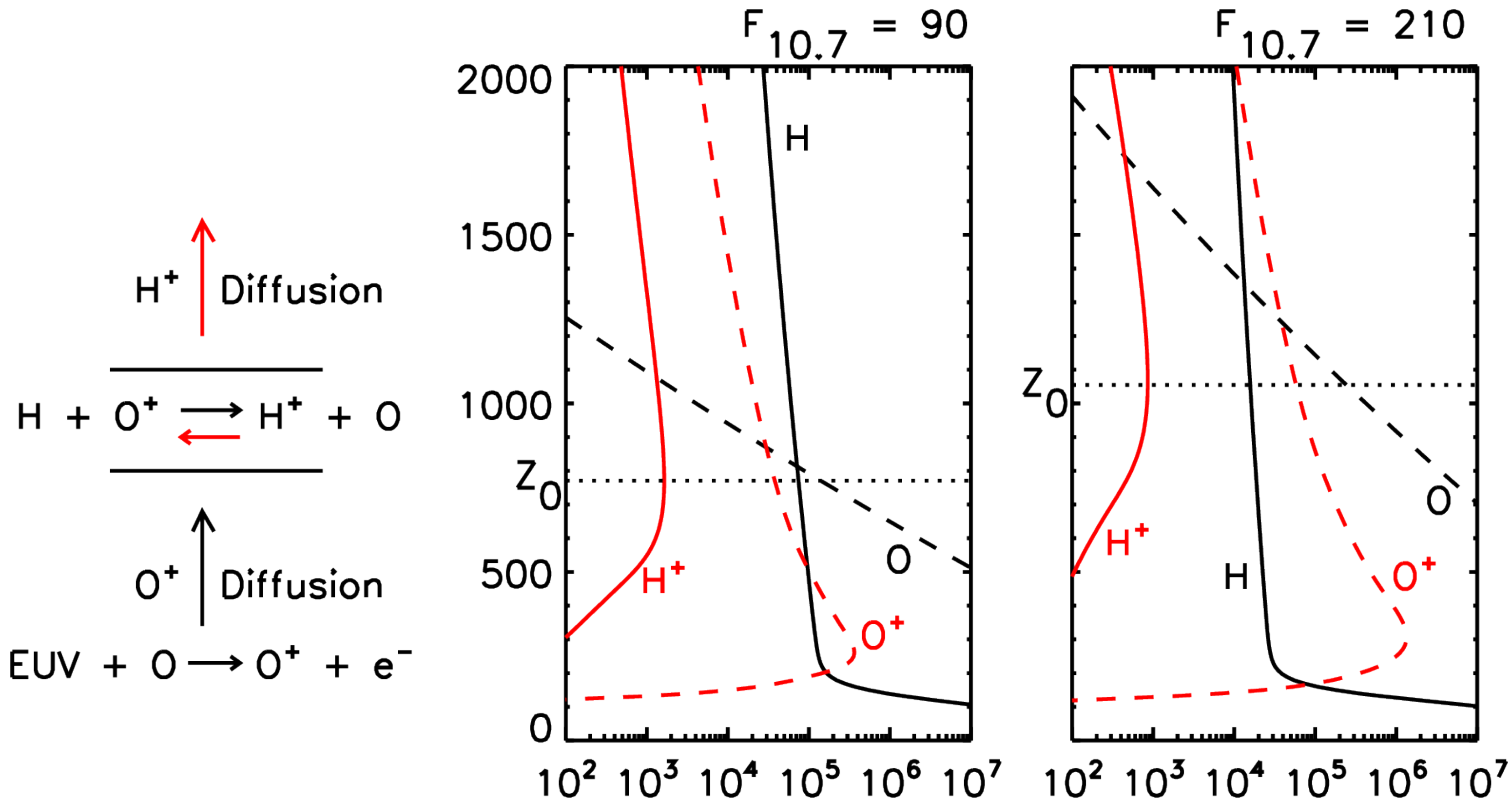

$$\phi[\mathrm{cm}^{-2}\mathrm{s}^{-1}] = 2.5 \times 10^{-11} T_n[\mathrm{K}]^{1/2} n_H[\mathrm{cm}^{-3}] n_{O^+}[\mathrm{cm}^{-3}] H_{O^+}[\mathrm{cm}]$$

The source height Z_0 is where H^+ is equally likely to react versus escape (two red arrows)

[Richards & Torr JGR, 1985]

Thermosphere densities affect H^+ outflow

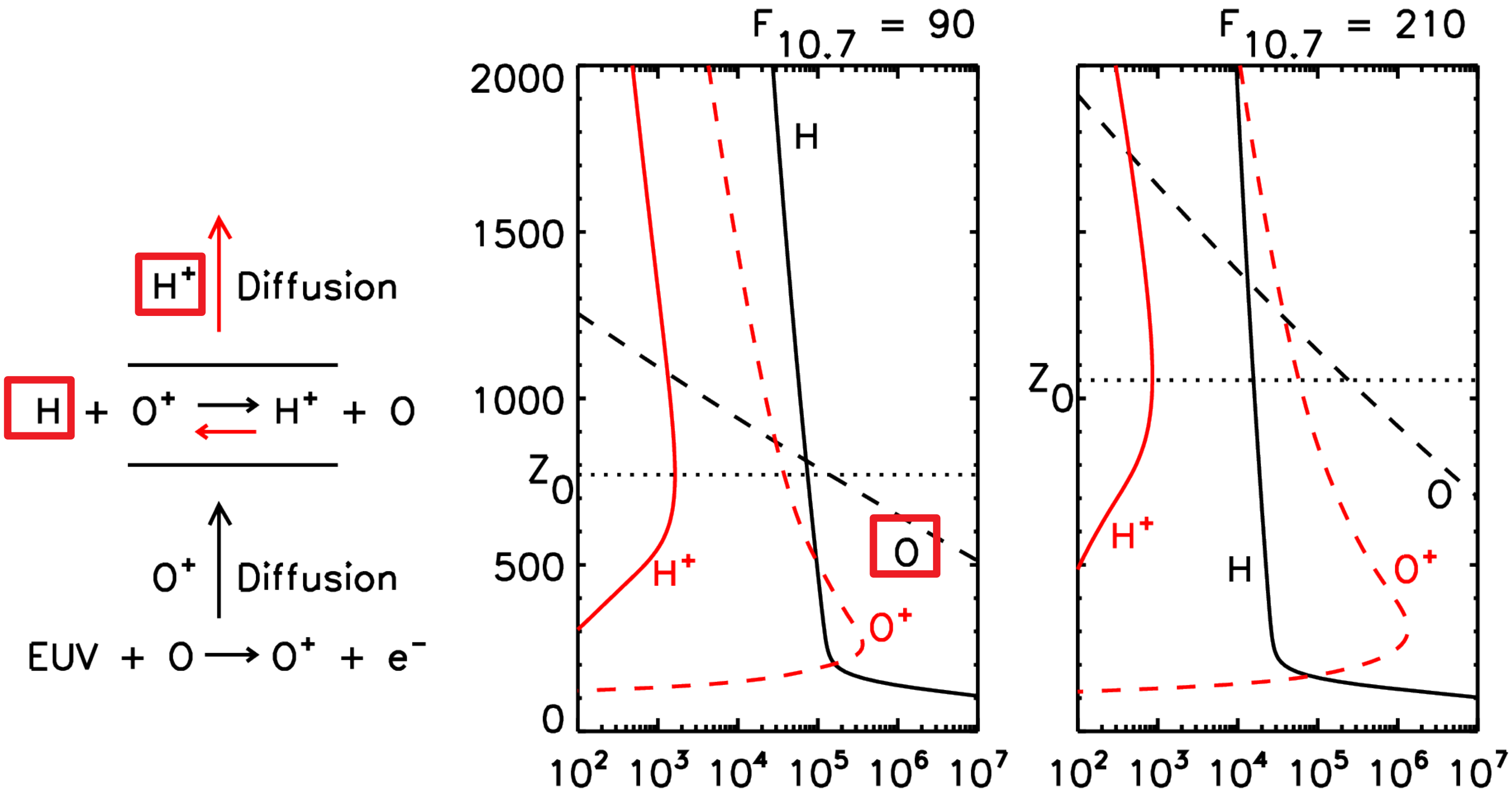

$$\phi[\mathrm{cm}^{-2}\mathrm{s}^{-1}] = 2.5 \times 10^{-11} T_n[\mathrm{K}]^{1/2} n_H[\mathrm{cm}^{-3}] n_{O^+}[\mathrm{cm}^{-3}] H_{O^+}[\mathrm{cm}]$$

- "Cold" is about 1 eV = 1.2 x 10^4 K
- Heat is needed for cold O^+ outflow

[Richards & Torr JGR, 1985]

H^+ Outflow is sensitive to O

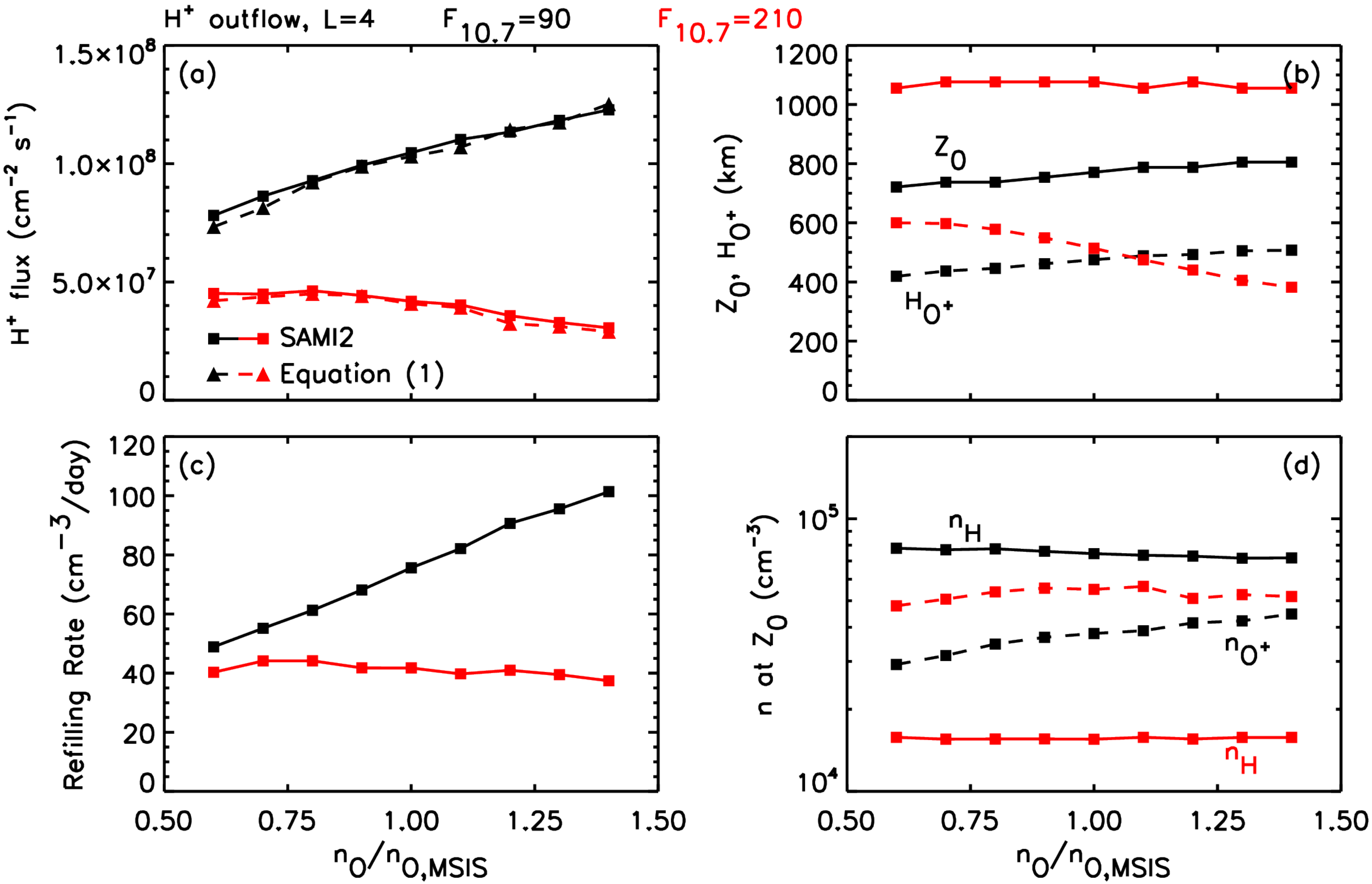

[Krall & Huba, JGR, 2019]

Measurement and modeling of 2001 day 328-336

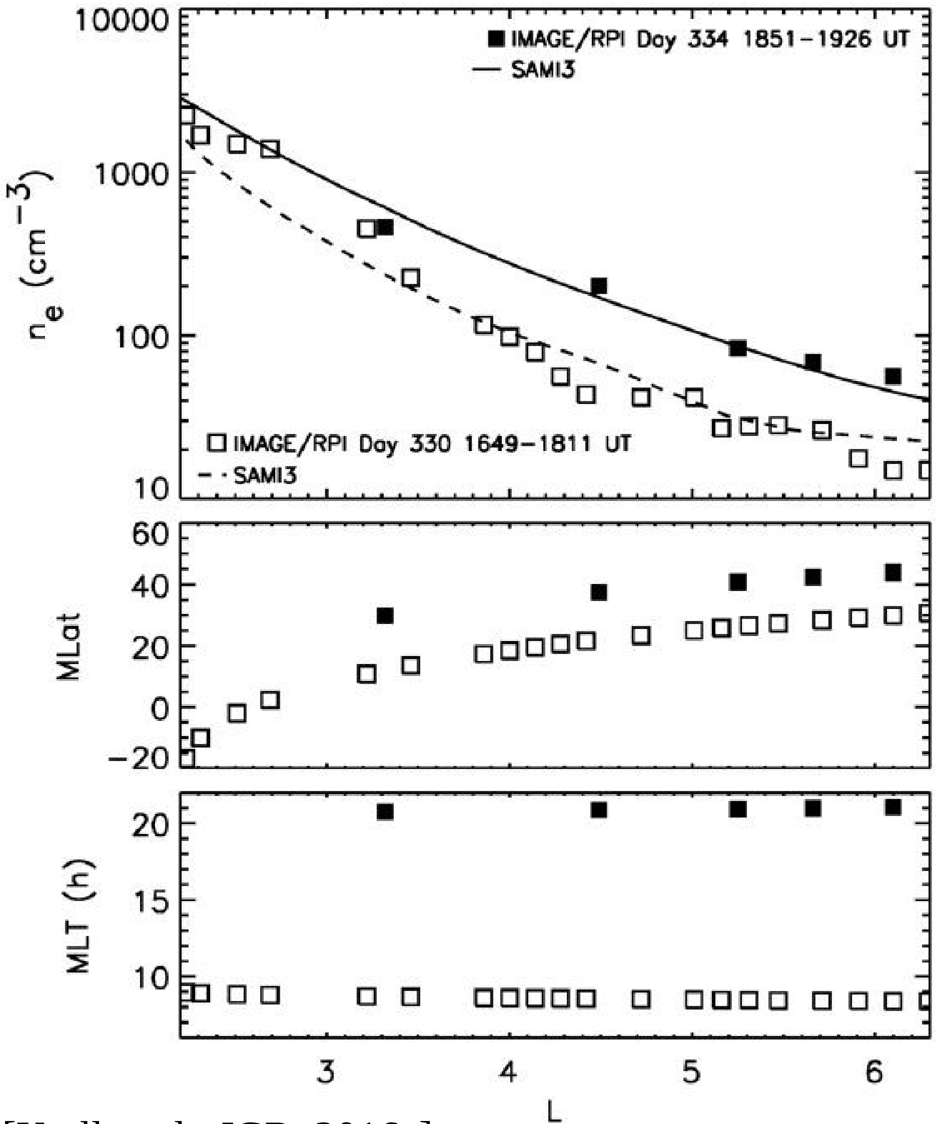

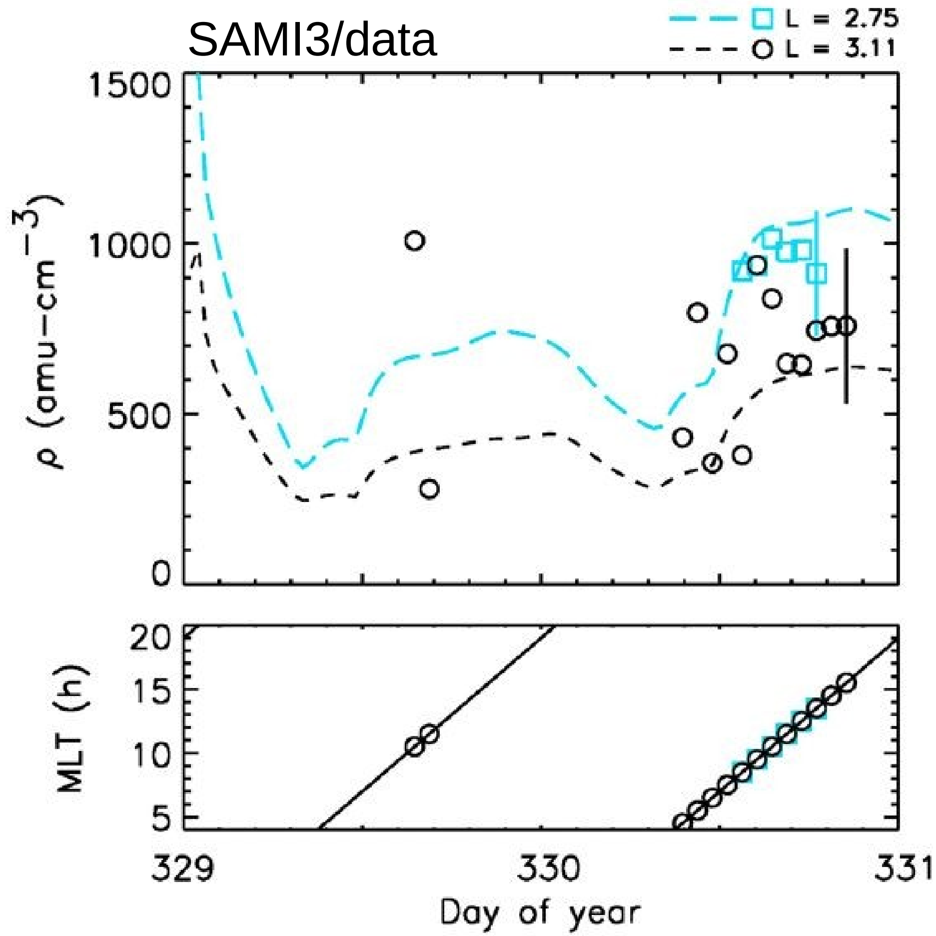

Mass density is from the MEASURE array, based on field-line resonance (FLR)

[Krall et al., JGR, 2016a]

Thermosphere variability and refilling

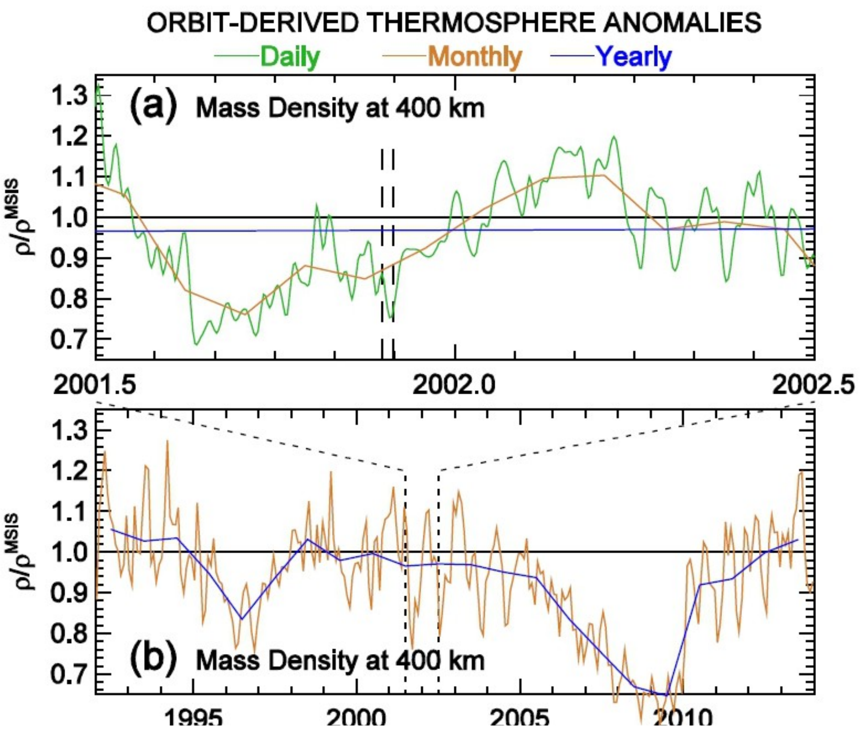

SAMI3/data: 26-30 November 2001

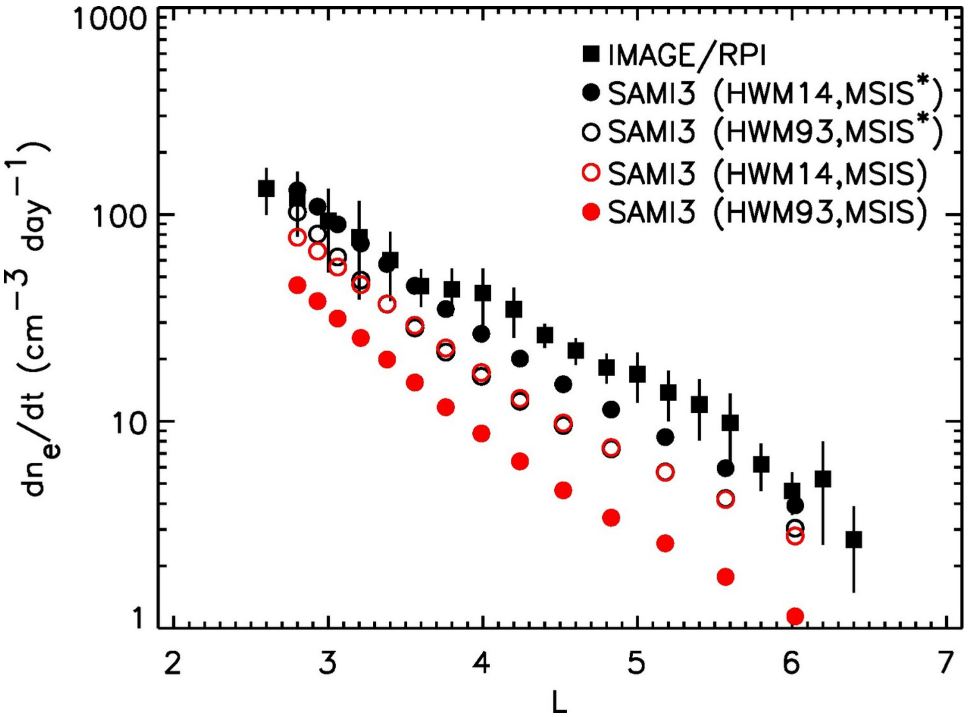

Green line: 4-day resolution O density based on satellite drag

With density corrected (MSIS*) and winds improved (HWM14),
The refilling rate is closer to the measurement

[Krall et al., JGR, 2016b]

IV. Ring current heating and the O+ torus

2015 October 7 storm

F10.7 = 80
F10.7a = 110

CIMI: ring current
SAMI3: ionosphere/plasmasphere
Potential: VSMC

CIMI: M.-C. Fok (NASA/GSFC)
A. Glocer (NASA/GSFC)

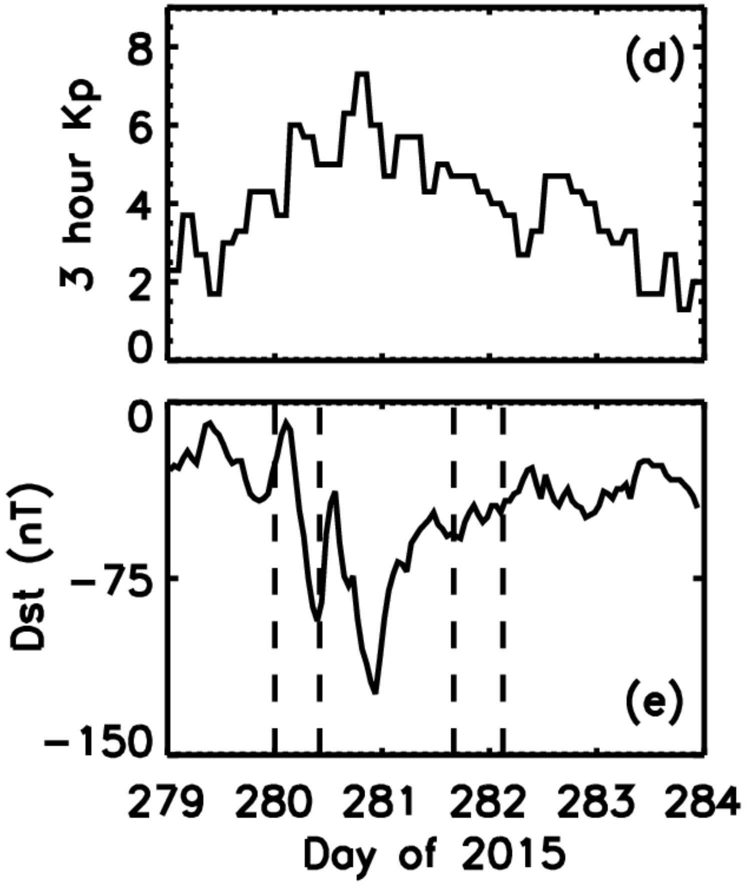

[Krall et al. GRL, 2020]

Ring current heating and the O^+ torus

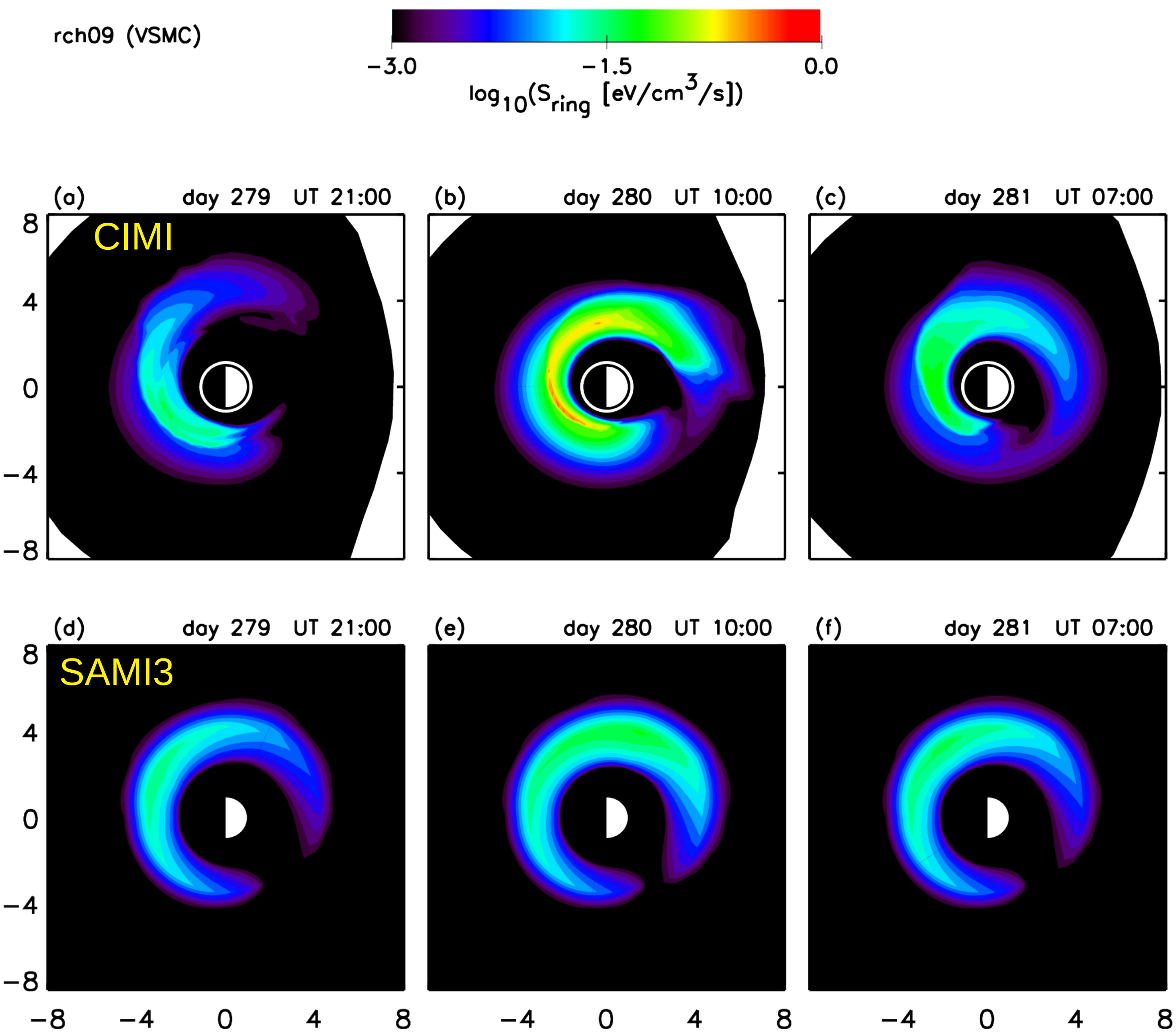

We added a heating term to the electron temperature equation to mimic CIMI heating.

Ring current heating and the O^+ torus

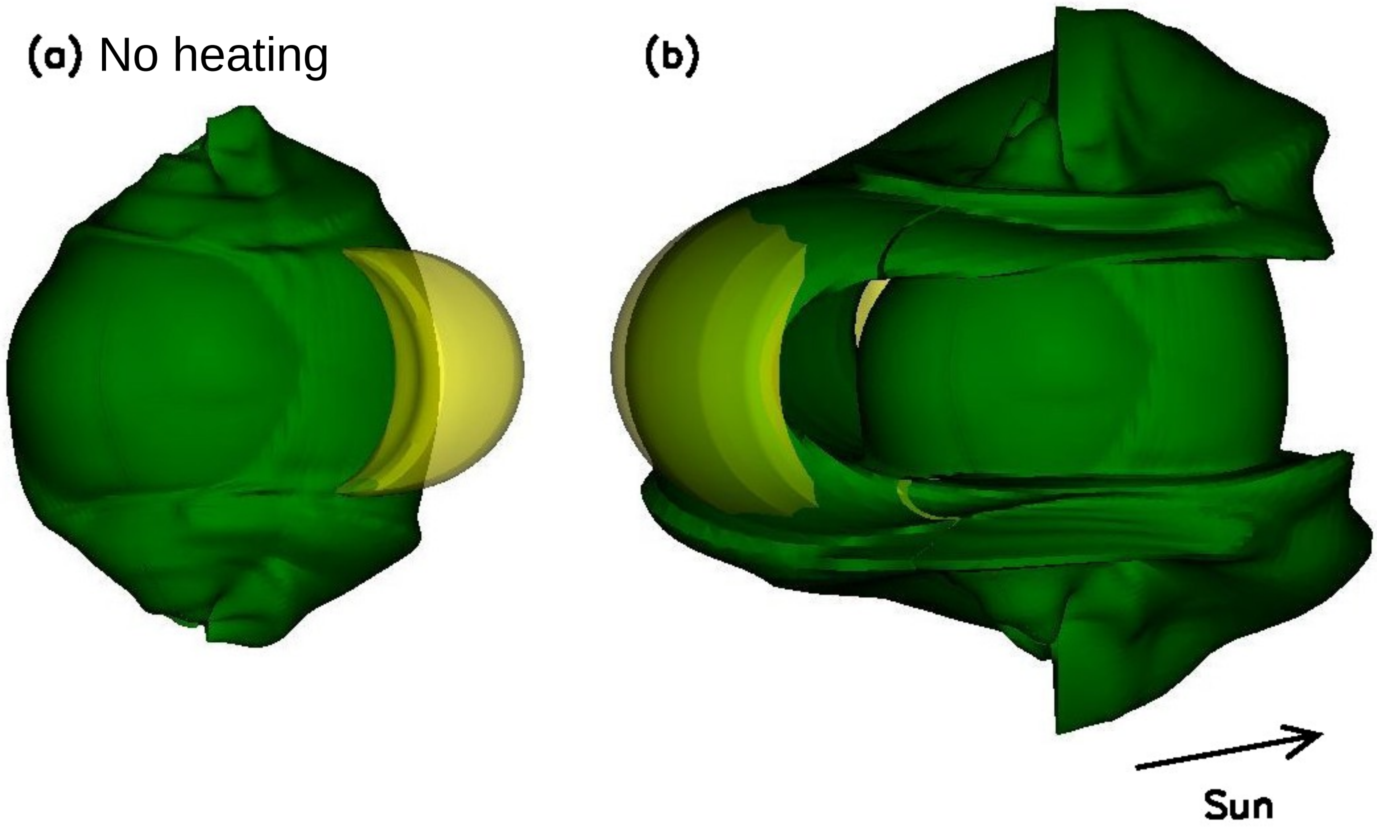

Green: O^+ density isosurface at 100 cm^{-3}

Yellow: e^- temperature surface at (a) 5.5×10^3 K, (b) 2×10^4 K

Ring current heating and the O^+ torus

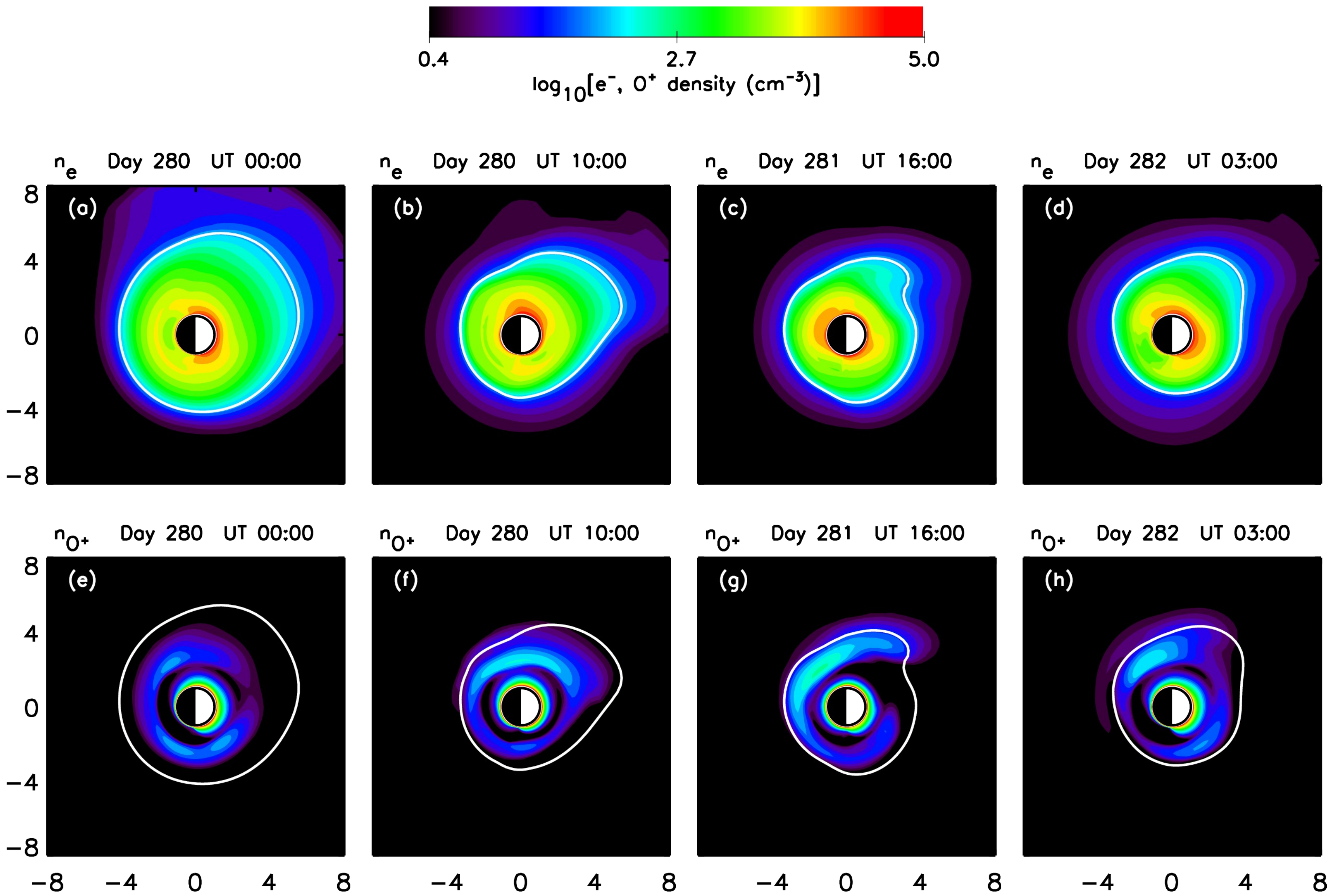

Model O⁺ torus is similar to observations

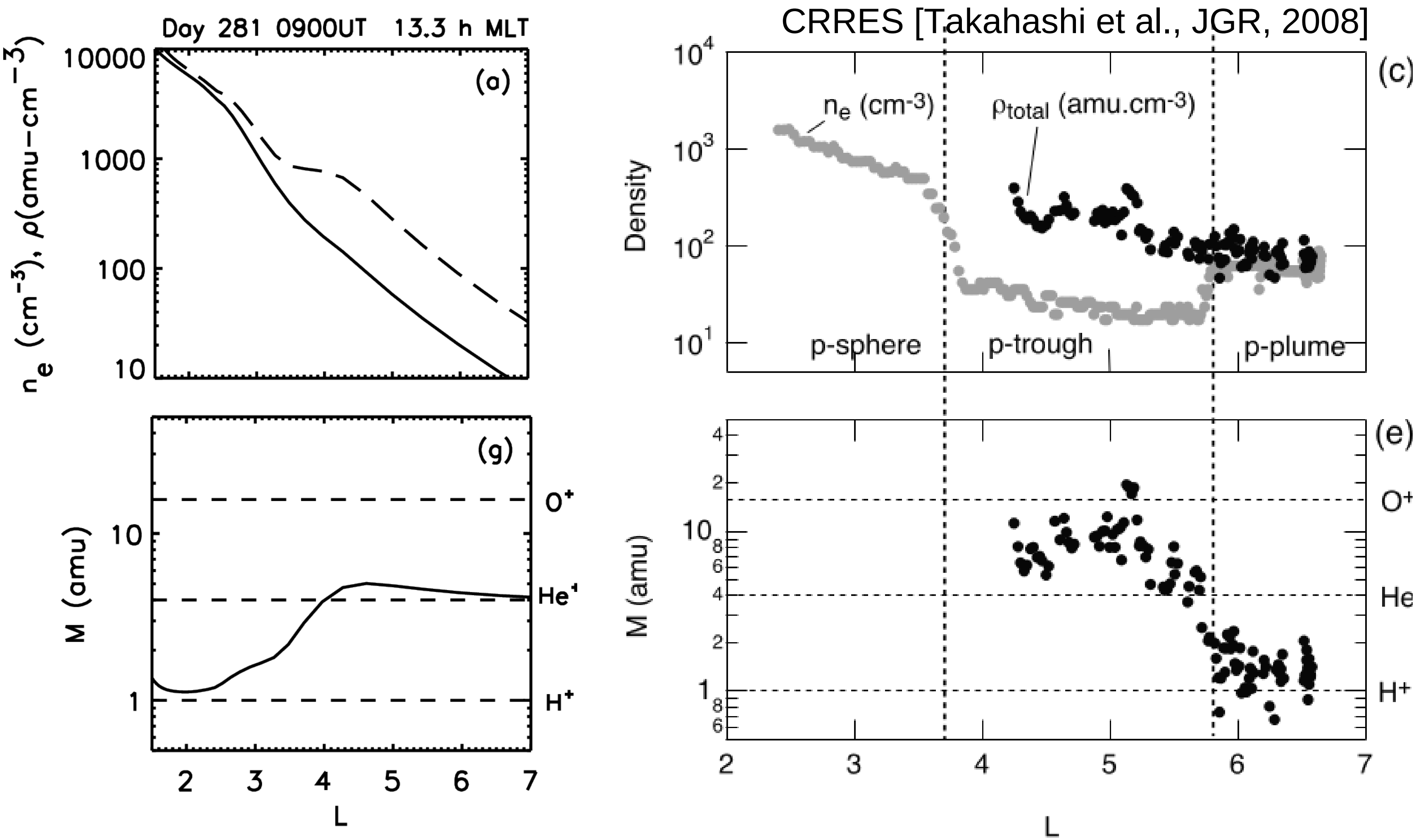

Model O^+ torus is similar to observations

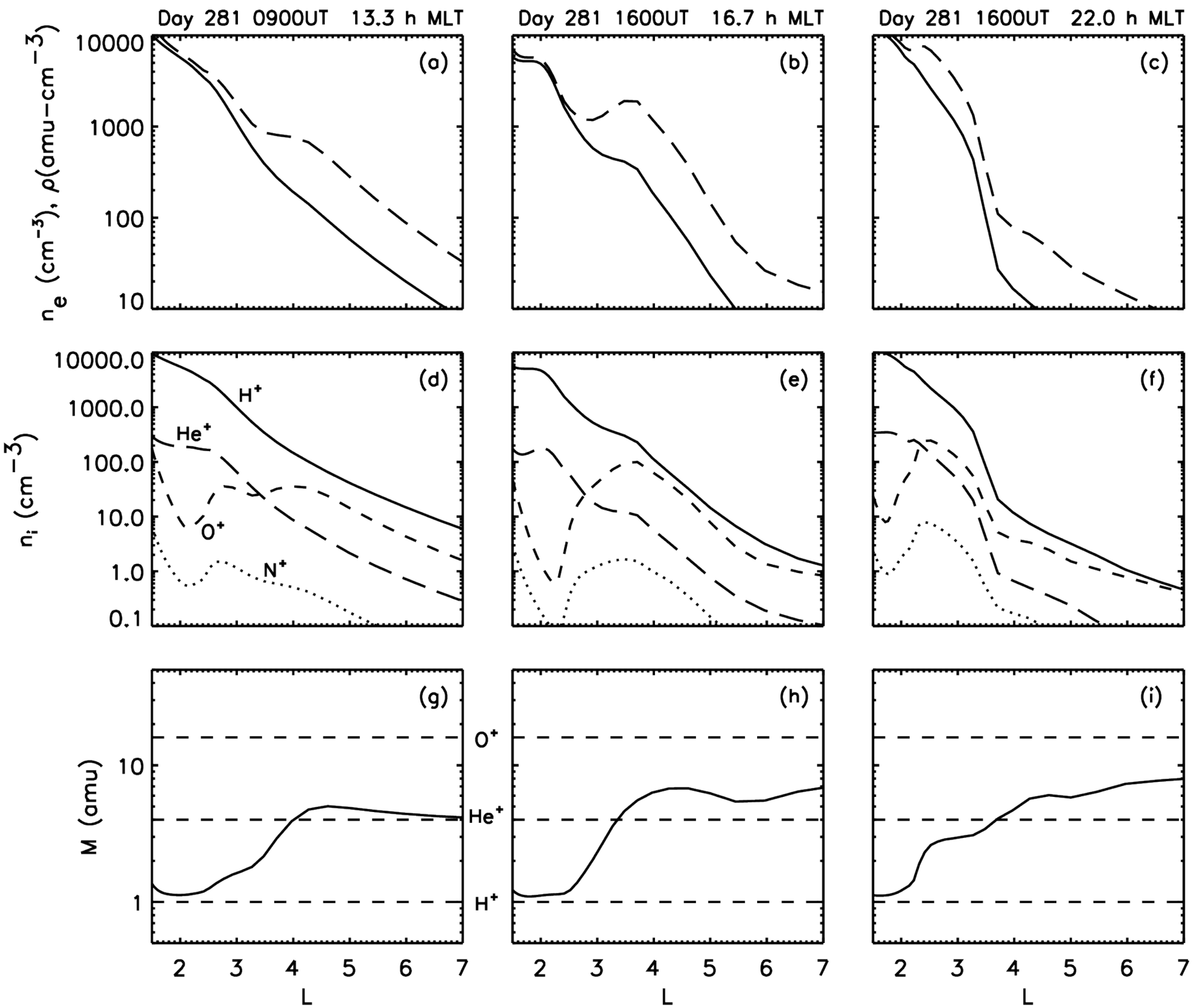

When the O^+ shell is present, the average mass is elevated inside the plasmapause

Model O^+ torus is similar to observations

[Nosé et al.,JGR, 2015]

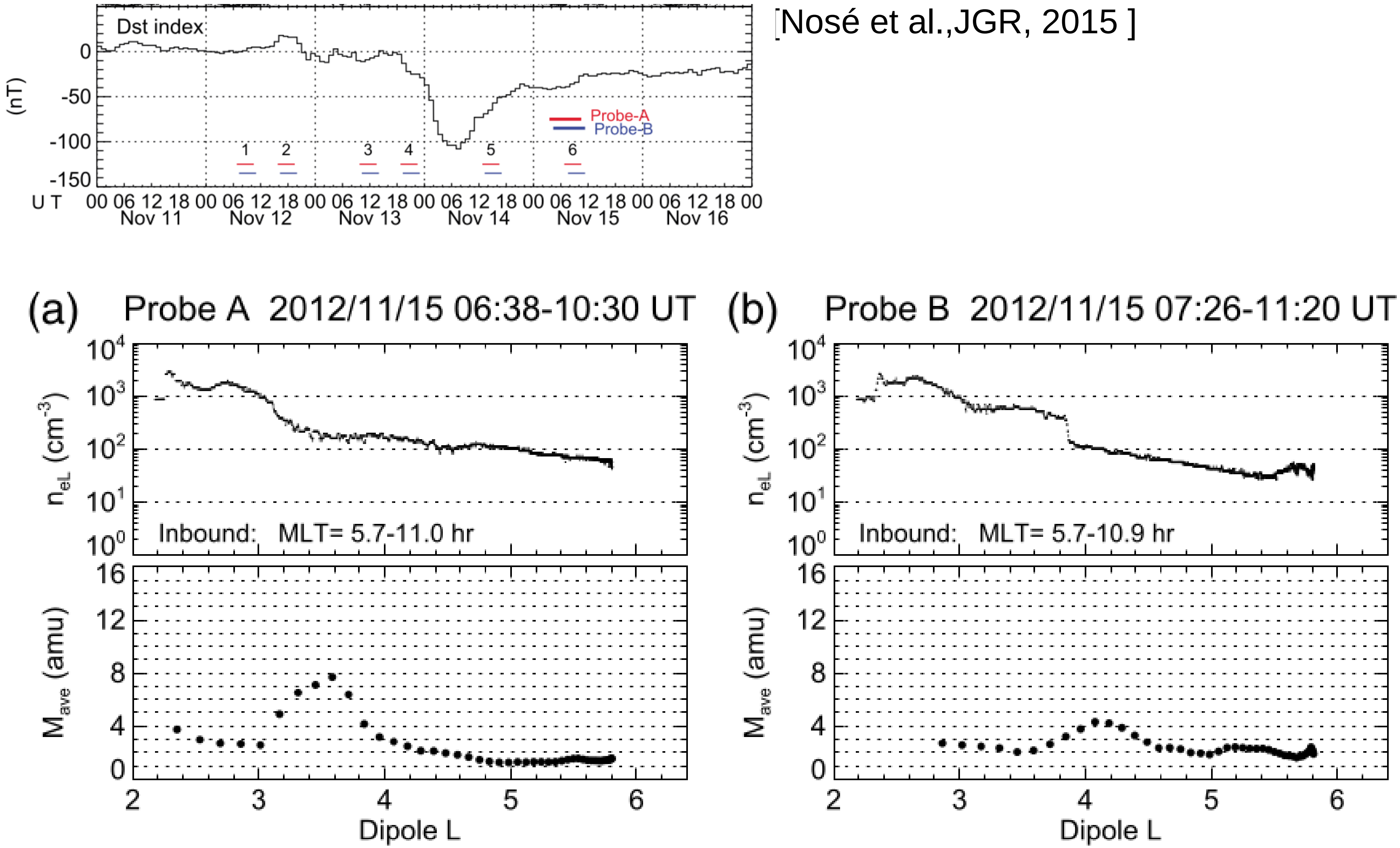

Model O^+ torus: composition

DE:RIMS [Roberts et al., JGR, 1987]

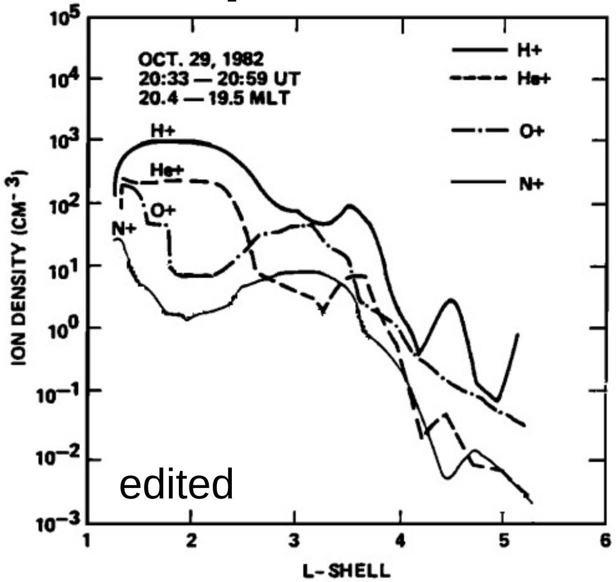

DE:RIMS [Horwitz et al., JGR, 1986]

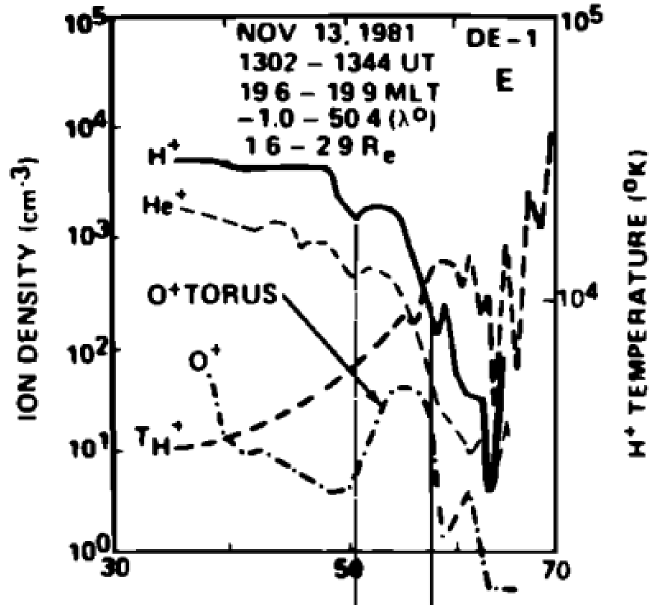

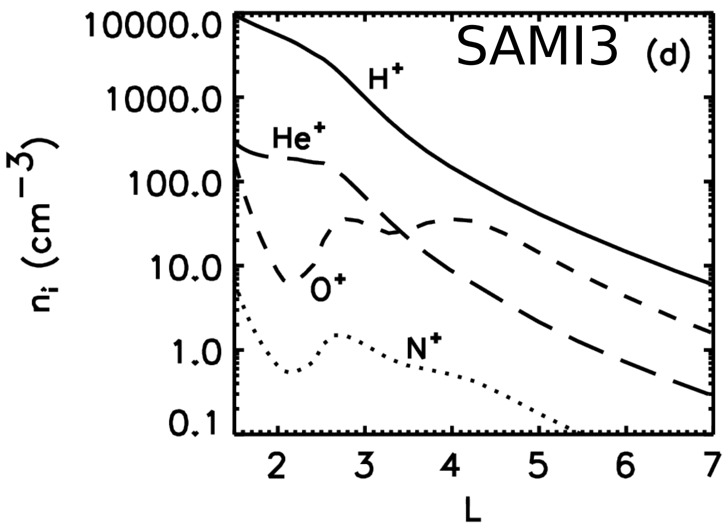

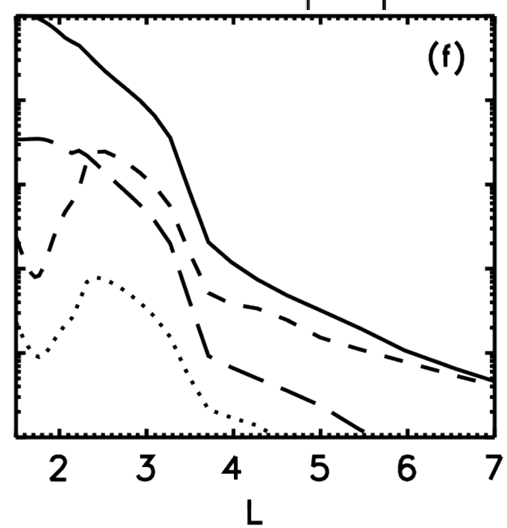

Where is the O+ torus/shell?

Chappell [1982]: “in the outer plasmasphere”

Horwitz et al. [1986]: “surrounding the inner plasmasphere” (refers to it as the O^+ O^{++} N^+ N^{++} torus/shell)

Roberts et al. [1987]: “almost always observed in the region of the plasmasphere just inside the plasmapause and has been seen at all local times.”

Direct heating of the ionosphere?

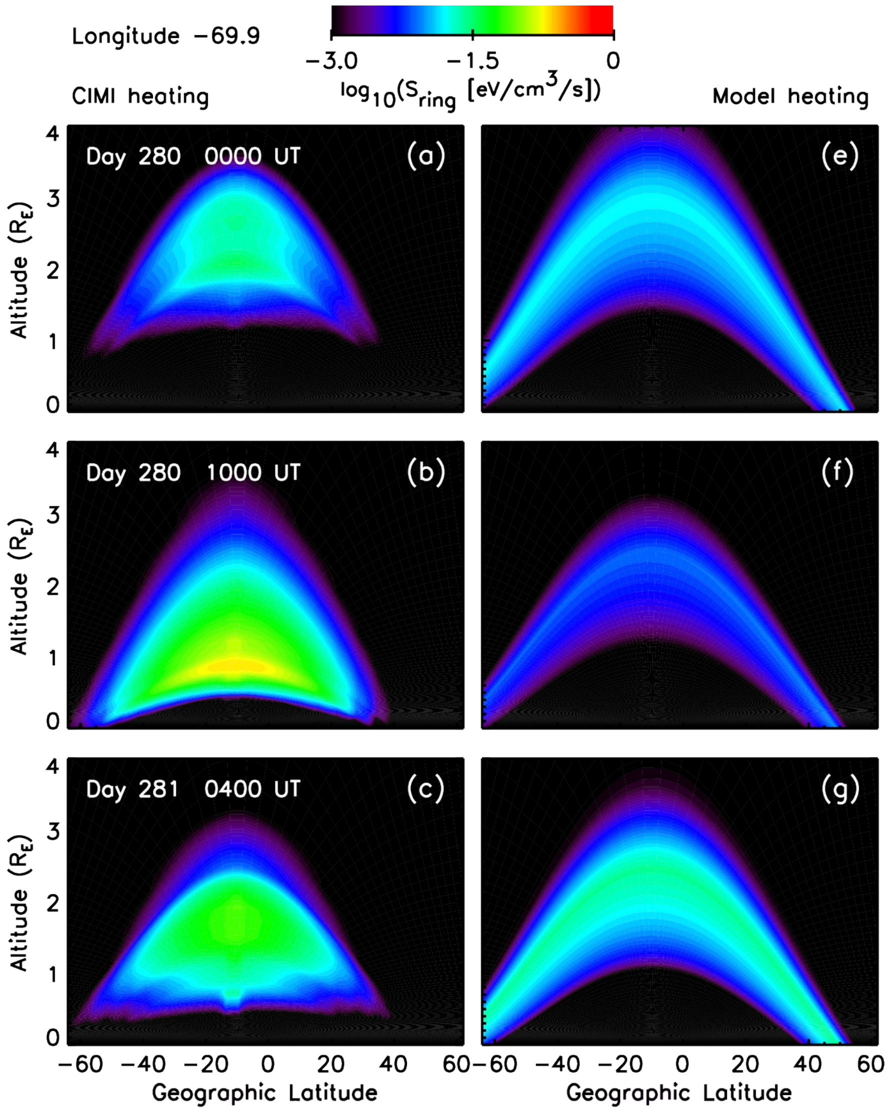

Left column: CIMI heating interpolated to the SAMI3 grid in magnetic coordinates.

Right column: the Dst-driven heating function used in initial tests of the ring-current-heating hypothesis.

[Krall et al., JGR, submitted]

Direct heating of the ionosphere?

Millstone Hill [Pavlov et al., Angeo, 1997]

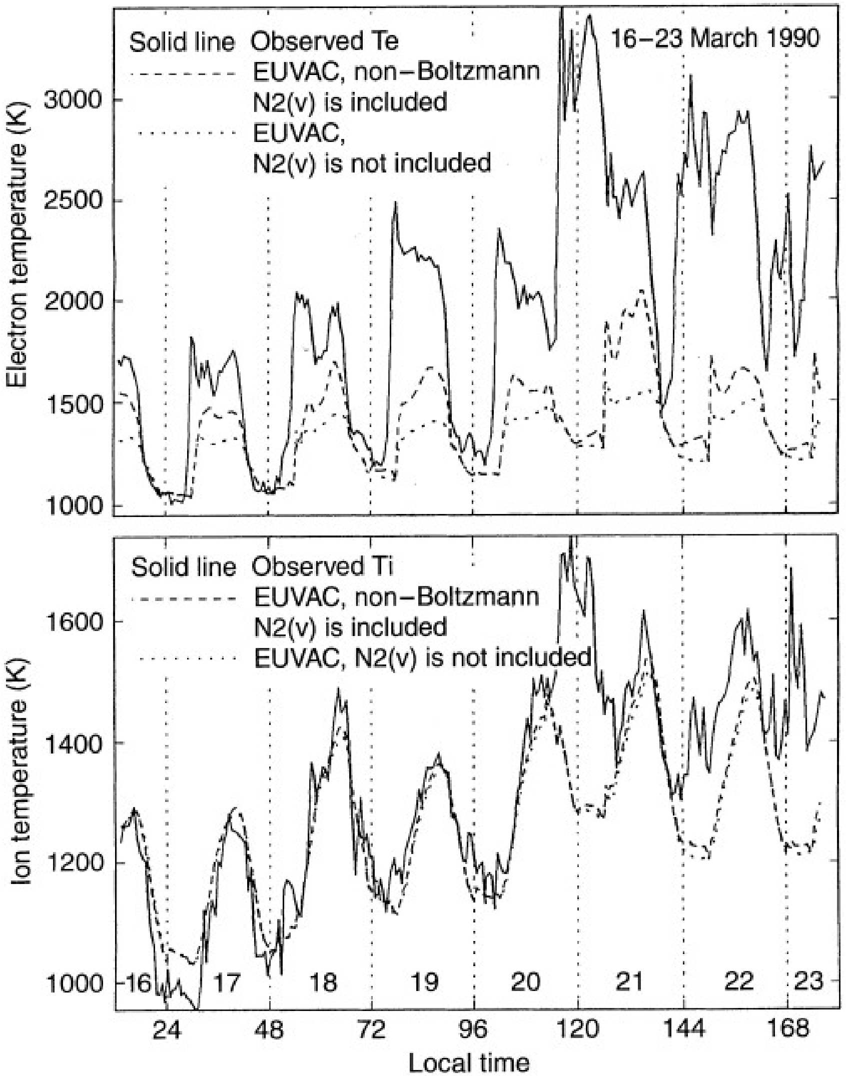

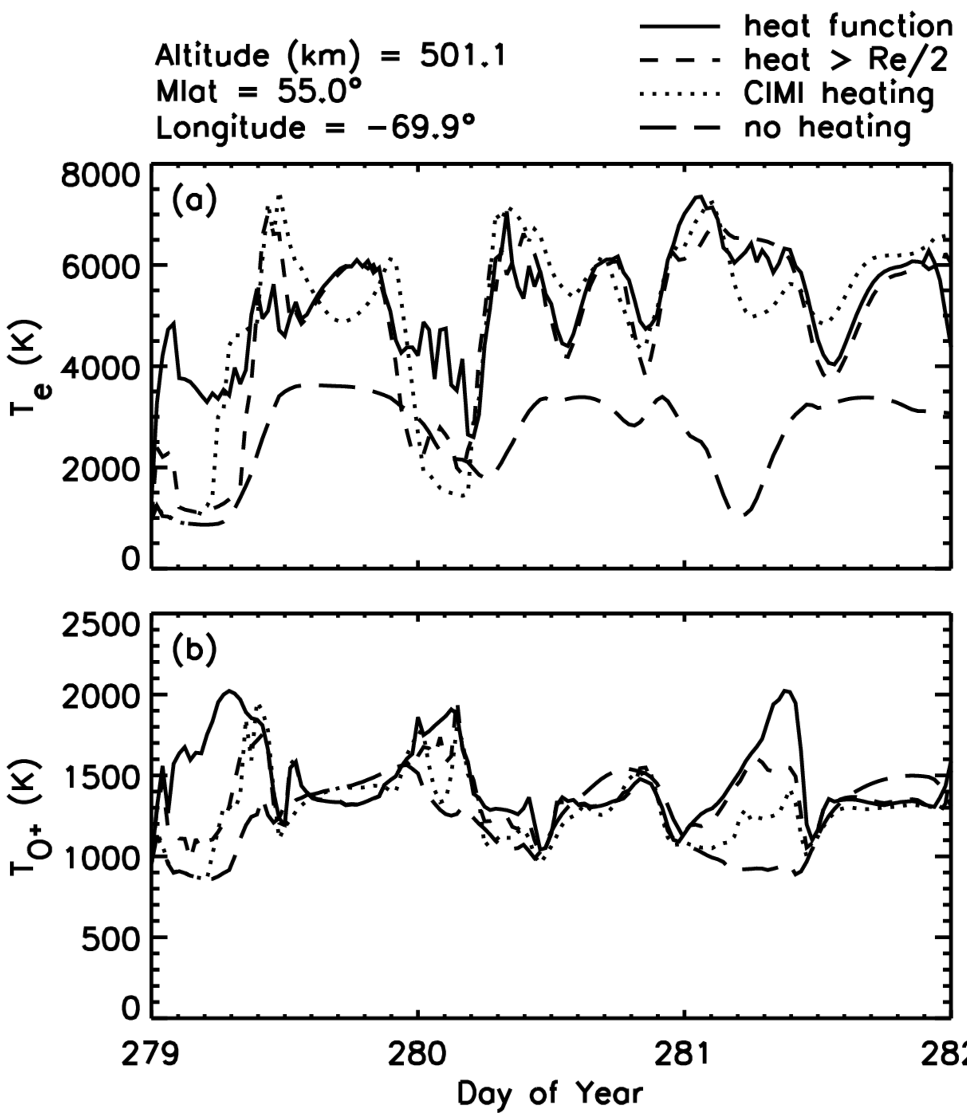

References

Chappell, C. R. (1982). Initial observations of thermal plasma composition and energetics from Dynamics Explorer-1. Geophysical Research Letters, 9(9), 929-932, doi:10.1029/294GL009i009p00929

Fok, M.-C., Buzulukova, N. Y., Chen, S.-H., Glocer, A., Nagai, T., Valek, P., & Perez, J. D. (2014), The Comprehensive Inner Magnetosphere-Ionosphere model, Journal of Geophysical Research: Space Physics, 119, 7522-7540, doi:10.1002/2014JA020239

Horwitz, J. L., Brace, L. H., Comfort, R. H., & Chappell, C. R. (1986), Dual-spacecraft measurements of plasmasphere-ionosphere coupling, Journal of Geophysical Research, 91(A10), 11,203-11,216, doi:10.1029/JA091iA10p11203

Huba, J. D., and Joyce, G. (2010), Global modeling of equatorial plasma bubbles, Geophys. Res. Lett., 37, L17104, doi:10.1029/2010GL044281.

Krall, J., Huba, J. D., Denton, R. E., Crowley, G., and Wu, T.-W. (2014), The effect of the thermosphere on quiet time plasmasphere morphology, J. Geophys. Res. Space Physics, 119, 5032– 5048, doi:10.1002/2014JA019850.

Krall, J., Huba, J. D., Jordanova, V. K., Denton, R. E., Carranza, T., and Moldwin, M. B. (2016a), Measurement and modeling of the refilling plasmasphere during 2001, J. Geophys. Res. Space Physics, 121, 2226-2248, doi:10.1002/2015JA022126.

Krall, J., Emmert, J. T., Sassi, F., McDonald, S. E., and Huba, J. D. (2016b), Day-to-day variability in the thermosphere and its impact on plasmasphere refilling, J. Geophys. Res. Space Physics, 121, 6889– 6900, doi:10.1002/2015JA022328.

Krall, J., & Huba, J. (2019), The effect of oxygen on the limiting H+ flux in the topside ionosphere, Journal of Geophysical Research: Space Physics, 124, 4509-4517, doi:10.1029/2018JA026252

References

Krall, J., Huba, J. D., & Fok, M.-C. (2020), Does ring current heating generate the observed O+ shell?, Geophysical Research Letters, 47, e2020GL088419, doi:10.1029/2020GL088419

Nosé, M., Oimatsu, S., Keika, K., Kletzing, C. A., Kurth, W. S., Pascuale, S. D., et al. (2015), Formation of the oxygen torus in the inner magnetosphere: Van Allen Probes observations, Journal of Geophysical Research: Space Physics, 120, 1182-1196, doi:10.1002/2014JA020593

Pavlov, A. V., & Buonsanto, M. J. (1997), Comparison of model electron densities and temperatures with Millstone Hill observations during undisturbed periods and the geomagnetic storms of 16–23 March and 6–12 April 1990, Annales Geophysicae, 15(3), 327-344, doi:10.1007/s00585-997-0327-4

Richards, P. G., & Torr, D. G. (1985). Seasonal, diurnal, and solar cyclical variations of the limiting H+ flux in the Earth's topside ionosphere. Journal of Geophysical Research, 90(A6), 5261–5268. https://doi.org/10.1029/JA090iA06p05261 Schrijver, C. J., Dobbins, R., Murtagh, W., & Petrinec, S. M. (2014). Assessing the impact of space weather on the electric power grid based

Roberts, W. T., Horwitz, J. L., Comfort, R. H., Chappell, C. R., Waite Jr., J. H., & Green, J. L. (1987), Heavy ion density enhancements in the outer plasmasphere, Journal of Geophysical Research, 92(A12), 13,499-13,512, doi:10.1029/JA092iA12p13499

Takahashi, K., Ohtani, S., Denton, R. E., Hughes, W. J., & Anderson, R. R. (2008), Ion composition in the plasma trough and plasma plume derived from a Combined Release and Radiation Effects Satellite magnetoseismic study, Journal of Geophysical Research, 113, A12203, doi:10.1029/2008JA013248

Thomas, E. G., Baker, J. B. H., Ruohoniemi, J. M., Clausen, L. B. N., Coster, A. J., Foster, J. C., and Erickson, P. J. (2013), Direct observations of the role of convection electric field in the formation of a polar tongue of ionization from storm enhanced density, J. Geophys. Res. Space Physics, 118, 1180–1189, doi:10.1002/jgra.50116

Extra: Plasmasphere electron content paradox

TEC (total electron content) is vertically-integrated density;
1 TECU = $10^{16}/m^2$.

TEC is not the number of electrons over a square meter.

pTEC can be defined as the TEC contribution between JASON altitude (1340 km) and GPS altitude (20,200 km).

pTEC is stronger at solar maximum [Lee et al., 2013; Shim et al 2017].

During solar maximum, the atmosphere expands, slowing refilling of the plasmasphere, leading to the “plasmasphere electron content paradox” [Krall & Huba, 2016].

TEC = iTEC + pTEC

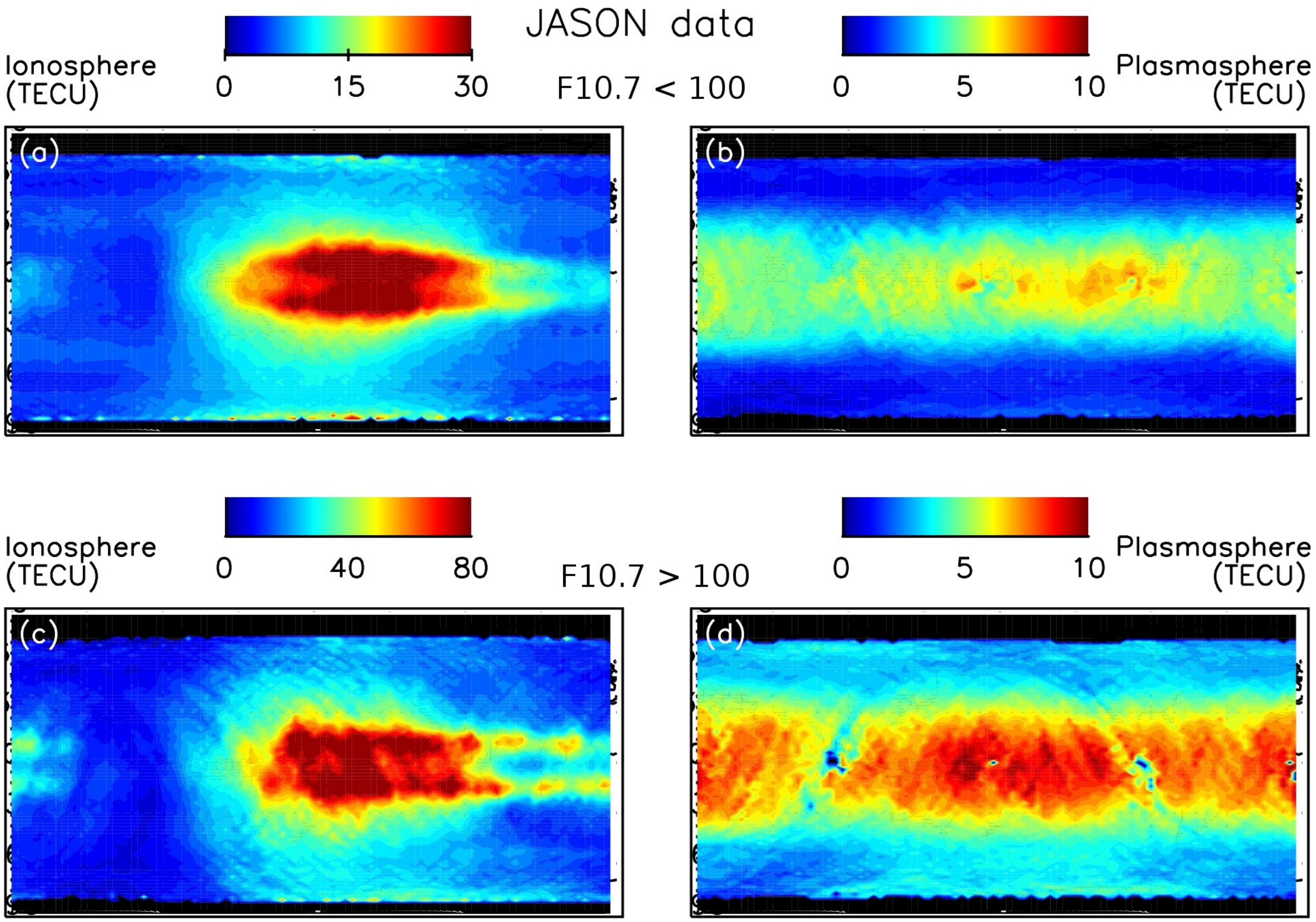

[Lee et al., JGR, 2013]

pTEC and iTEC data courtesy of H.-B. Lee

F10.7 is EUV index (80, 160 for solar min, max)

Measured pTEC result based on data from 2002-2009.

Refilling is slower at solar max

[Rasmussen et al., 1993, Plan. Space Sci.]

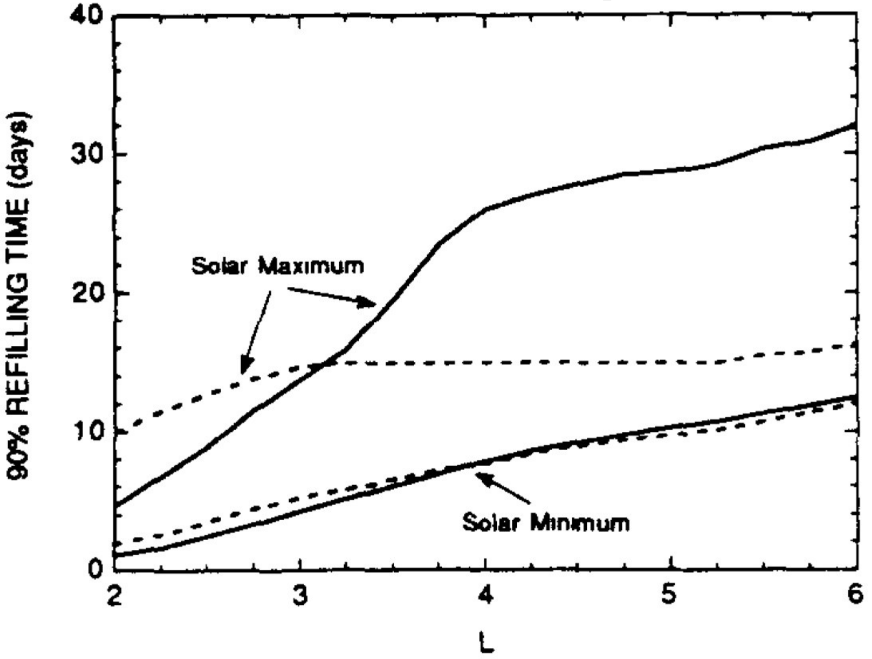

It is well-known that post-storm plasmasphere refilling rates fall with solar activity.

Refilling times are longer at solar maximum.

The paradox is that refilling rates fall with increasing solar activity while pTEC increases with increasing solar activity.

SAMI3/MSIS* agrees with observations

[Krall & Huba, JGR, 2016]

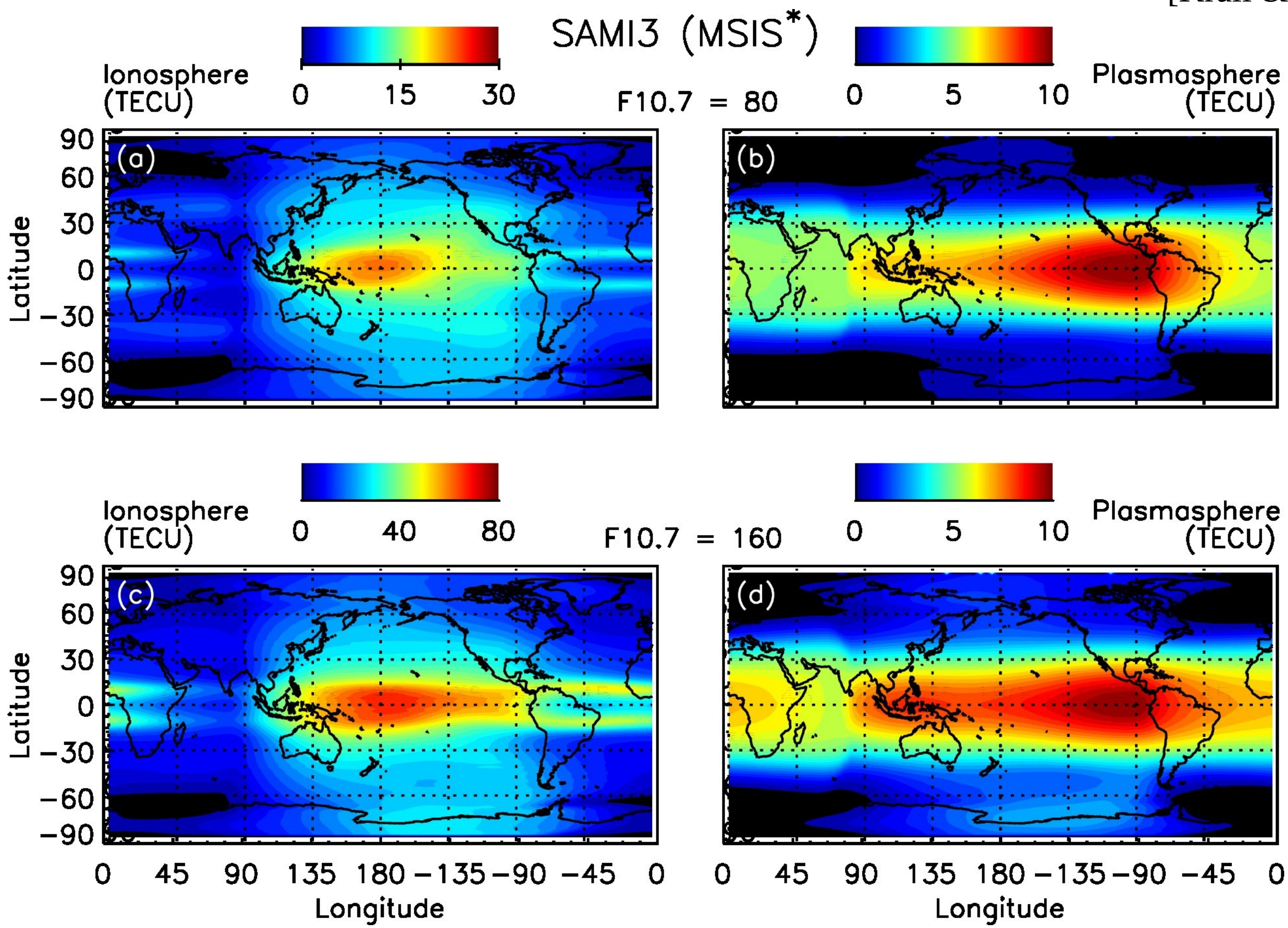

As in measurements, both TEC and pTEC increase with F10.7.

SAMI3/MSIS* reproduces the paradox

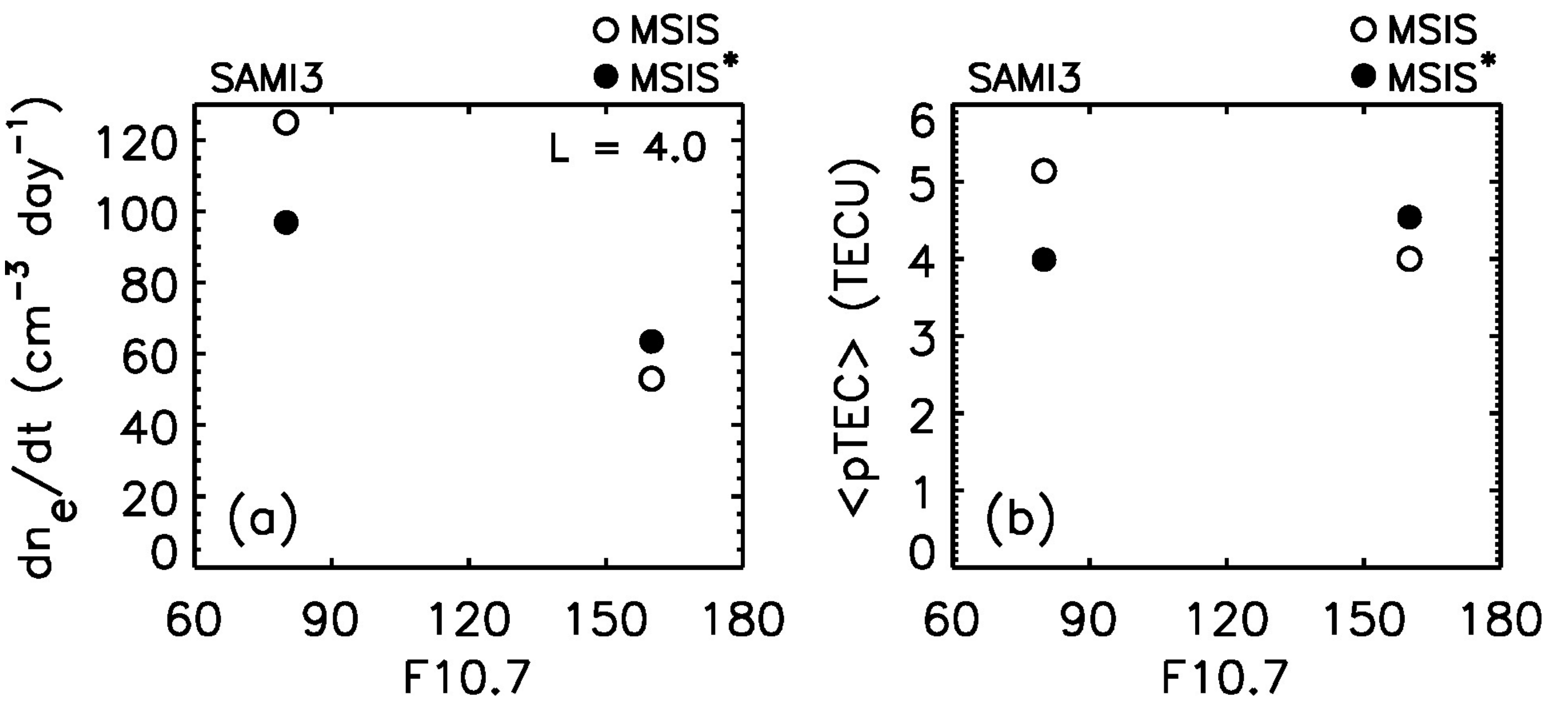

SAMI3 with the MSIS* modified atmosphere (black dots) reproduces the paradox: refilling rates fall vs F10.7 while pTEC increases vs F10.7.

pTEC is sensitive to the thermosphere

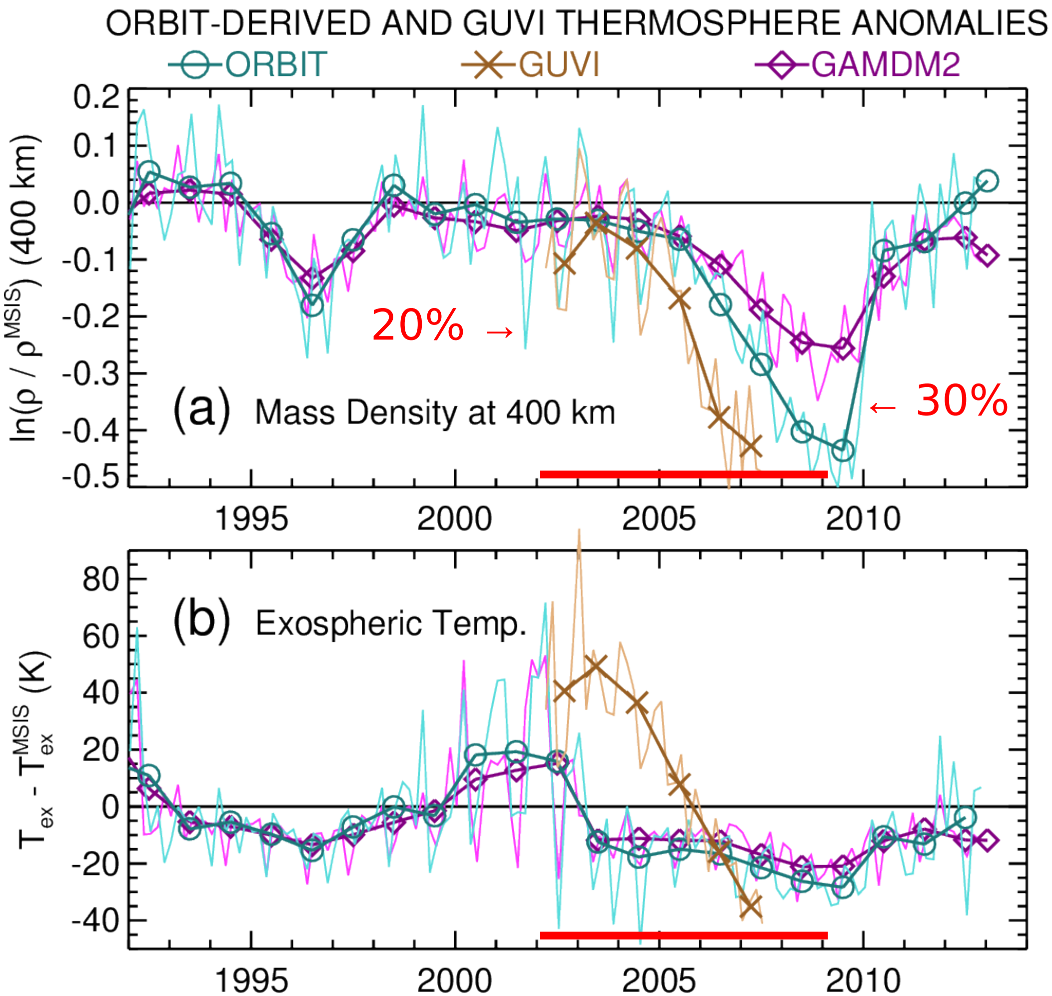

Measured density variations of 20% are common.

Fine lines are 61-day averages (Yaw cycle).

[Emmert et al., JGR, 2014]

TEC dominated by near-Earth electrons

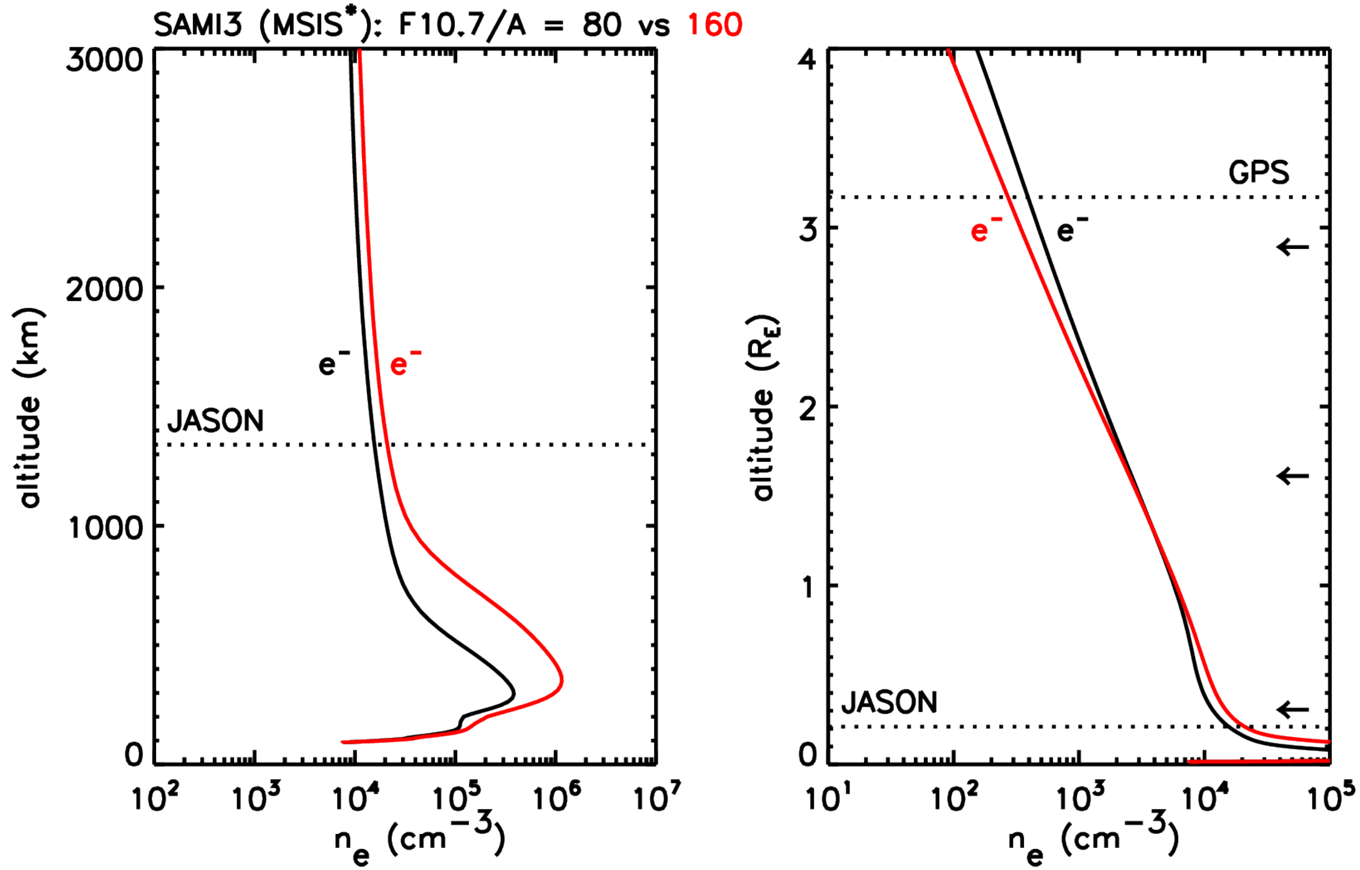

Electrons at geocentric radius 1.3 R_E contribute 4 times as much as electrons at 2.6 R_E and 9 times as much as at 3.9 R_E.

pTEC isn't strongly affected by storms

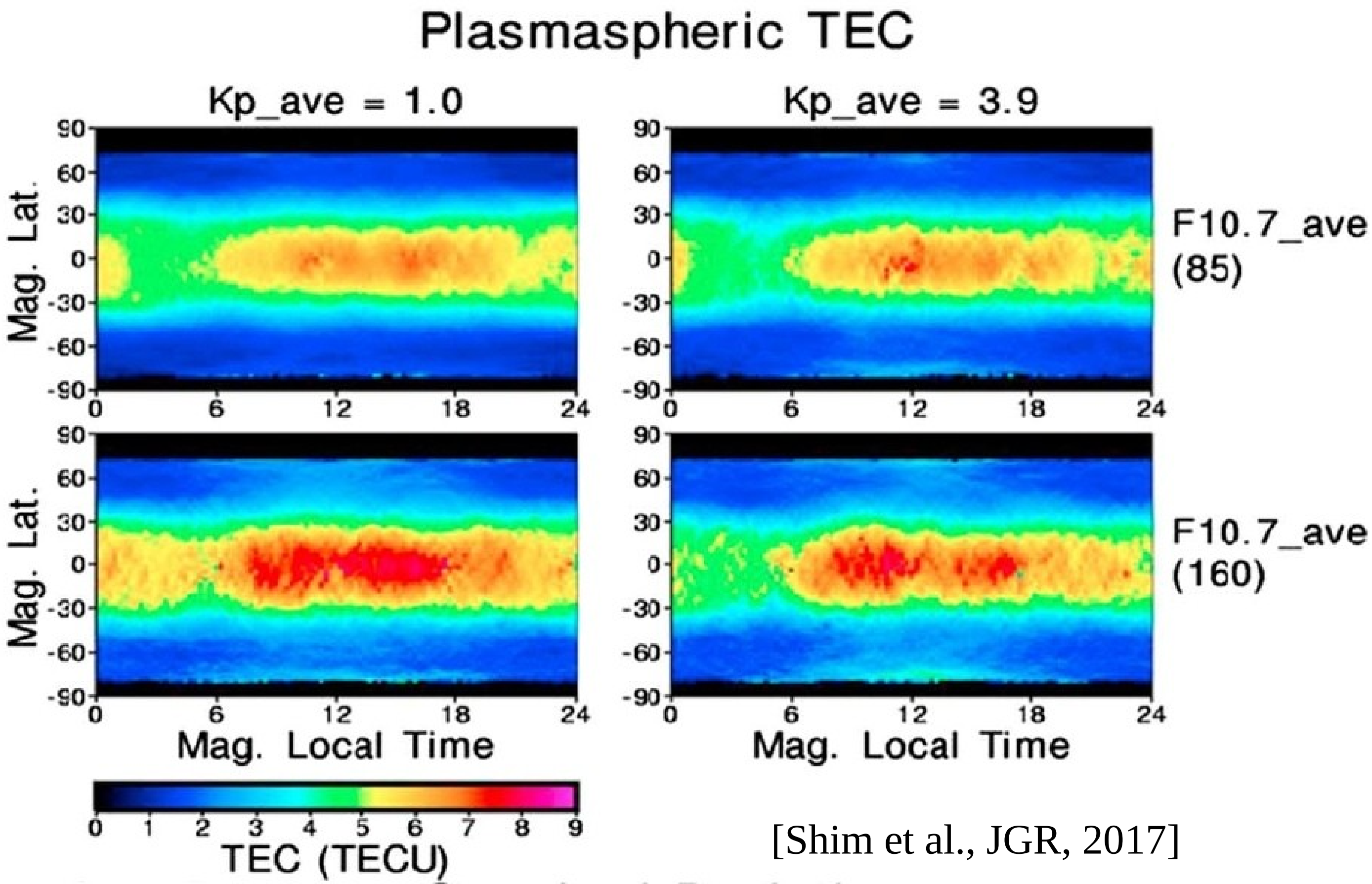

[Shim et al., JGR, 2017]

Related to the fact that pTEC gives more weight to near-Earth electrons, it is also not strongly affected by storms.

More references

Emmert, J. T., S. E. McDonald, D. P. Drob, R. R. Meier, J. L. Lean, and J. M. Picone (2014), Attribution of interminima changes in the global thermosphere and ionosphere, Journal of Geophysical Research: Space Physics, 119 (8), 6657-6688, doi:10.1002/2013JA019484

Krall, J., and J. D. Huba (2016), The plasmasphere electron content paradox, J. Geophys. Res. Space Physics, 121, 8924–8935, doi:10.1002/2016JA023008

Lee, H.-B., G. Jee, Y. H. Kim, and J. S. Shim (2013), Characteristics of global plasmaspheric TEC in comparison with the ionosphere simultaneously observed by JASON-1 satellite, J. Geophys. Res. Space Physics, 118 (2), 935-946, doi:10.1002/jgra.50130

Rasmussen, C. E., S. M. Guiter, and S. G. Thomas (1993), Two-dimensional model of the plasmasphere: refilling time constants, Planet. Space Sci., 41, 35-43, doi:10.1016/0032-0633(93)90015-T

Shim, J. S., G. Jee, and L. Scherliess (2017), Climatology of plasmaspheric total electron content obtained from Jason 1 satellite, J. Geophys. Res. Space Physics, 122, 1611–1623, doi:10.1002/2016JA023444